

Submitted tanggal 8 April 2021

Manuscript submitted to International Journal of Photoenergy Inbox x



**International Journal of Photoenergy** <marina.adel@hindawi.com> [Unsubscribe](#)  
to me ▾

Apr 8, 2021, 10:37 AM ☆ ↶ ⋮



Hindawi

Dear Dr. Siregar,

Congratulations, the manuscript titled "Fabrication of dye-sensitized solar cells (DSSC) using Mg-doped ZnO as photoanode and extract of rose myrtle (*Rhodomyrtus tomentosa*) as natural dye" has been successfully submitted to International Journal of Photoenergy.

We will confirm this submission with all authors of the manuscript, but you will be the primary recipient of communications from the journal. As submitting author, you will be responsible for responding to editorial queries and making updates to the manuscript.

In order to view the status of the manuscript, please visit the manuscript details page.

Thank you for submitting your work to International Journal of Photoenergy.

[MANUSCRIPT DETAILS](#)

Kind regards,

# Fabrication of dye-sensitized solar cells (DSSC) using Mg-doped ZnO as photoanode and extract of rose myrtle (*Rhodomyrtus tomentosa*) as natural dye

Nurdin Siregar<sup>1\*</sup>, Motlan<sup>1</sup>, Jonny Haratua Panggabean<sup>1</sup>, Makmur Sirait<sup>1</sup>, Juniastel Rajagukguk<sup>1</sup>, Noto Susanto Gultom<sup>1</sup>, Fedlu Kediri Sabir<sup>2</sup>.

<sup>1</sup>Department of Physics, Faculty of Mathematics and Natural Sciences, State University of Medan, Jl. Willem Iskandar Pasar Medan Estate, Medan 20221, Indonesia

<sup>2</sup>Department of Applied Chemistry, School of Applied Natural Science, Adama Science and Technology University, P.O. Box 1888, Adama, Ethiopia

\*Corresponding author: [siregarnurdin@unimed.ac.id](mailto:siregarnurdin@unimed.ac.id)

## ABSTRACT

A dye-sensitized solar cell (DSSC) device using Mg-doped Zn thin films as photoanode and fruit extract of rose myrtle (*Rhodomyrtus tomentosa*) as the natural dye was investigated. The effect of annealing temperatures (400-550 °C) on the films of photoanode was systematically studied using X-ray diffractometer (XRD), UV-Visible Near Infrared (UV-Vis NIR) Spectrophotometer, scanning electron microscopy (SEM), and energy dispersive spectroscopy (EDS). XRD confirm that all sample has the wurtzite hexagonal with crystallite size of 25 nm. The SEM images reveal that the surface of Mg-doped ZnO thin film is nanosphere. A higher annealing temperature leads to a larger grain size. The bandgap energy slightly increases by increasing the annealing temperature. The dye sensitizer of rose myrtle (*Rhodomyrtus tomentosa*) has a strong absorption at the visible light region. The maximum efficiency of the DSSC device is 3.53% with Mg-ZnO photoanode annealed at 500 °C.

**Keywords:** *Dye Sensitized Solar Cell, Mg-doped ZnO, sol-gel spin coating, natural dye*

## 1. INTRODUCTION

The higher demands of renewable energy continually increase every single year due to its eco-friendliness and regenerality. Solar cells have been well known to convert solar energy to electricity for decades. However, the conventional solar cells are still competitive in the high price market with complicated fabrication process. Dye-sensitized solar cells (DSSCs), is one of the most promising solar cell types to generate renewable energy with a low-cost material and simple fabrication [1-3]. The working principal of DSSCs is the utilized during the solar irradiation to convert into electric current. After irradiation, the dye sensitizer harvests light and causes an electron to promote the conduction band leaving a hole in the valence band. There are numerous pigments of plant leaves, fruits, and flowers that have the potential to utilize in DSSCs. The variety of pigments with different width of light harvesting ranges and degree of absorptivity in UV-Visible spectrum results in differences in the performance of DSSCs. The molecules of the dye can be anchored into the surface areas of the semiconductor to form Lewis acid-base types of interaction to enhance electron transfer from HOMO of the dye molecule (pigment) to the conduction band of the semiconductor (anode) [4-7]. In particular, zinc oxide (ZnO) semiconductor plays a role as a photoanode to improve the conducting interface layer and to enhance the power conversion efficiency (PCEs). According to the literatures, ZnO has high electron mobility, wide bandgap (3.37eV), and large exciton binding energy of 60 meV [8]. Magnesium (Mg) is one of the metals that used in many applications such as refractory materials, optical and heating apparatus [9, 10]. This material also has special properties to block the electron due to of its wide bandgap [11].

There are several methods to grow thin films on the substrate, such as molecular beam epitaxy, metal organic chemical vapor deposition, plasma enhanced chemical deposition, sputtering method, spray pyrolysis, atomic layer deposition, pulse laser deposition, electron beam evaporation, and sol-gel spin coating techniques [12]. Each of those methods has advantages and disadvantages. Nevertheless, sol-gel spin coating approach is a simple, cheap, and effective method that employs simple equipments to

synthesize ZnO thin films [13]. During sol-gel spin coating for ZnO thin film production, parameters such as concentration of precursor solution, annealing temperature, film morphology, and dopant growth need to be controlled [14].

In this work, the photoanodes of Mg-doped ZnO thin films were prepared by Sol-gel spin coating; and the fruit extract of *Rhodomyrtus tomentosa* was used as sensitizer. DSSC devices were fabricated from pigments of *Rhodomyrtus tomentosa* fruit extract, platinum coated counter electrode, and the photoanode. The effect of different annealing temperatures of photoanode on the efficiency of DSSC was investigated.

## **2. EXPERIMENTAL SECTION**

### **2.1. Synthesis of Mg-doped ZnO thin films**

Mg-doped ZnO thin films were fabricated using sol-gel spin coating technique. Typically, Zinc Acetate dehydrate and magnesium chloride (2%) were dissolved in isopropanol under continuous stirring. After 10 min, 1.7 mL diethanolamine was added slowly into the solution. After refluxing process at 90 °C for about 2 hours, the gel was dropped on top of FTO glass and spinned at 5000 rpm for 60 s. After the drying process, the samples were annealed at different temperatures of 400, 450, 500, and 550°C for 5 hours.

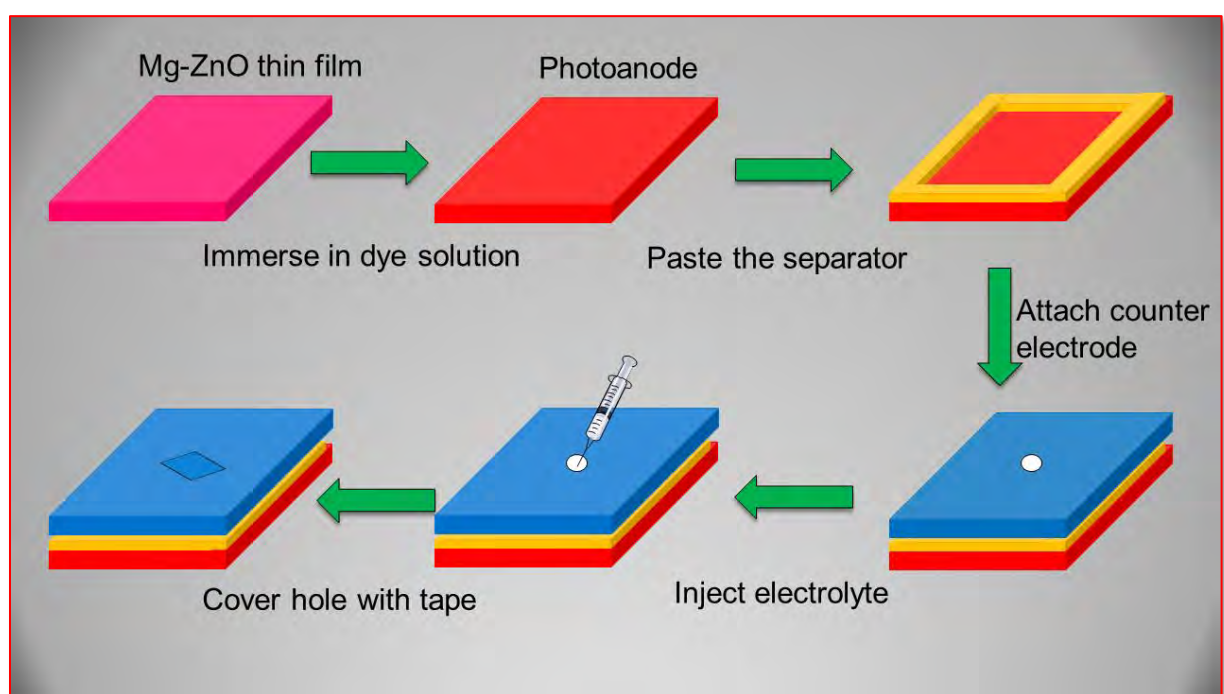
### **2.2. Extraction of natural dyes**

About 50 grams of *Rhodomyrtus tomentosa* fruit was ground using a mortar. After being moved into a beaker glass, 25 mL DI water, 21 mL ethanol, and 4 mL acetic acid were added and then stirred to form a homogenous solution. The solution was then covered with aluminum foil to avoid photooxidation and soaked at room temperature for 24 h. Finally, the solid and liquid parts were separated using filter paper. The filtered solution of *Rhodomyrtus tomentosa* fruit extract was ready to be used as sensitizer in DSSCs.

### **2.3. Fabrication of DSSC**

Figure 1 illustrates the schematic fabrication of DSSC. First, the as-prepared Mg-doped ZnO thin film was used as the photoanode electrode. Natural-dye sensitized from *Rhodomyrtus tomentosa* fruit extract was

adsorbed on the top of Mg-doped ZnO photoanode by immersing it into the extracted dye solution for several hours. After that, it was taken out and washed with ethanol to remove the unadsorbed dye and dried in the oven. The platinum coated on the glass FTO was used as the counter electrode. The DSSCs were assembled by attaching the photoanode and the counter electrode using thermoplastic sealant surlyn as glue and separator. And then heated at 80 °C to let the surlyn perfectly attach to the electrodes. The electrolyte was injected through a tiny hole on the counter electrode. Finally, that hole was covered with transparent tape.



**Figure 1.** Schematic of the fabrication of DSSC using Mg-doped ZnO photoanode and fruit extract of *Rhodomyrtus tomentosa*.

## 2.4. Characterizations

To observe the surface morphology of Mg-doped ZnO thin films annealed at different temperatures, a scanning electron microscope (JEOL-6500) analysis was performed at an accelerating voltage of 15 kV.

The X-ray diffraction of Mg-doped ZnO thin films were analyzed using an X-ray diffractometer (LabX XRD-6100, Shimadzu) with Cu K $\alpha$  ( $\lambda=1.54$  Å). The transmittance and absorbance spectra were recorded using a UV-Vis NIR spectrophotometer. The efficiency of the DSSC was measured using an I-V measurement (Keithly Source Measure Unit) system by irradiating a photoanode electrode with a light source. Several data such as open-circuit voltage ( $V_{oc}$ ), short circuit current density ( $J_{sc}$ ), and fill factor (FF) were recorded. Then, the efficiency was determined using equations (1) and (2)

$$\eta = \frac{P_{max}}{P_{in}} \times 100\% = FF \frac{J_{sc} \times V_{oc}}{P_{in}} \times 100\% \quad (1)$$

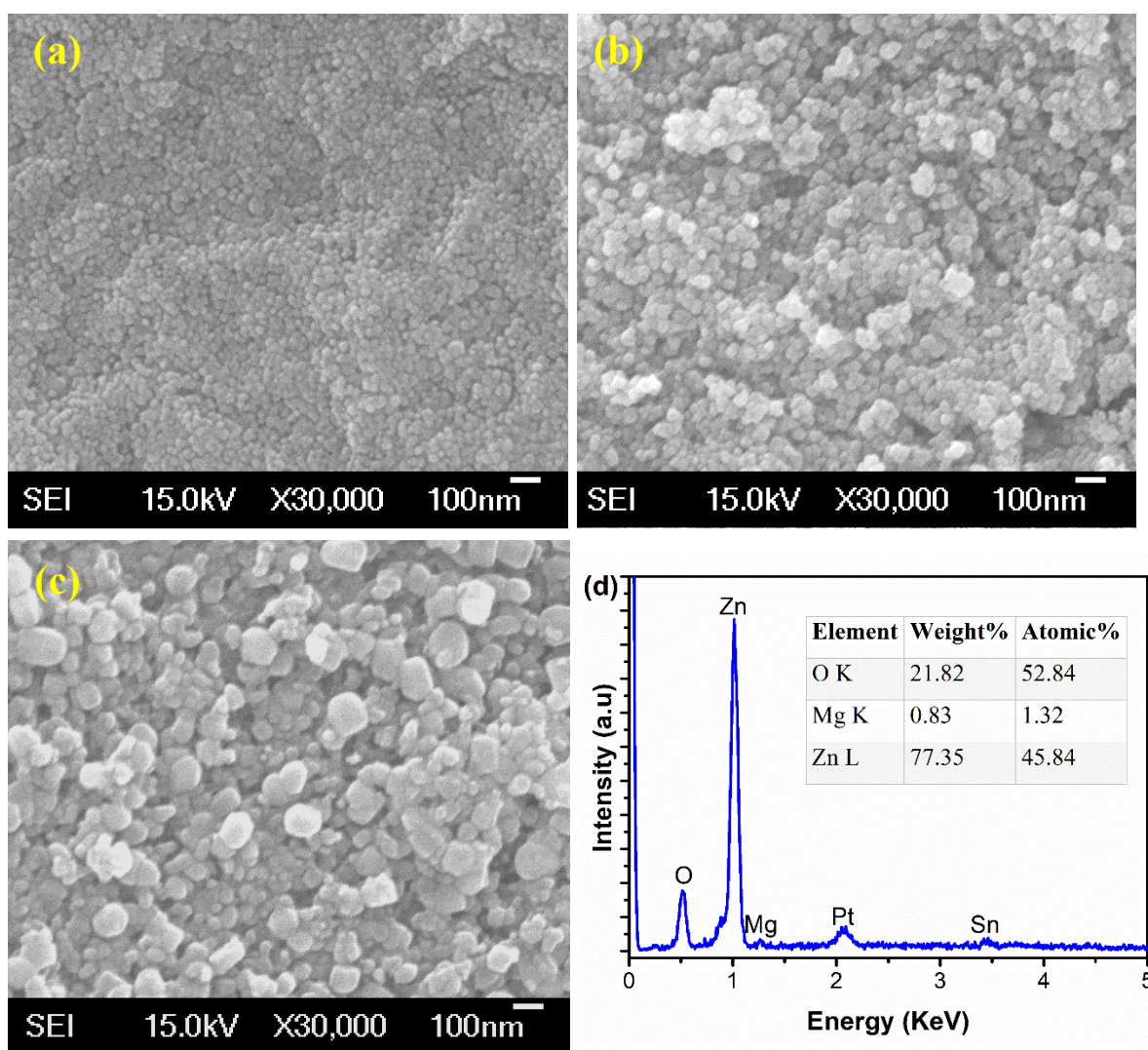
$$FF = \frac{J_{max} \times V_{max}}{J_{sc} \times V_{oc}} \quad (2)$$

### 3. RESULTS AND DISCUSSION

#### 3.1. Electron microscope analysis

The surface morphology of Mg-doped ZnO with variation of annealing temperature was investigated using a field-emission scanning electron microscope. With a magnification of 30 k times, the clear top view images of Mg-doped ZnO thin films can be clearly observed in Figure 2. The surface microstructure of Mg-doped ZnO at different annealing temperatures looks similar to nanosphere shapes. It was clearly observed that by increasing the annealing temperature, the grain size was monotonically increased. To calculate the grain size precisely, further analysis was conducted using software. The results of J image analysis confirmed that the average particle sizes for Mg-doped ZnO thin films annealed at 400, 500, and 550 °C were  $30 \pm 5$ ,  $53 \pm 9$ , and  $82 \pm 17$  nm, respectively. A larger particle size at a higher annealing temperature was reasonable. It could be explained due to a higher driving force from thermal energy that leads to a faster particle growth through Ostwald ripening mechanism. Our findings also well agree with some previous reports [15, 16].

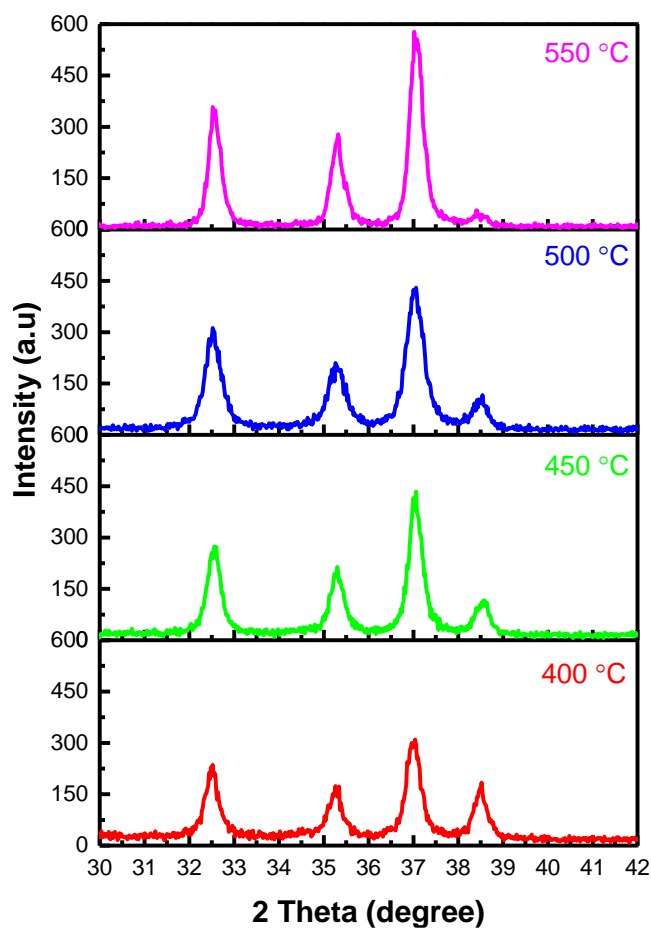
Figure 2d shows the representative energy disperse spectroscopy (EDS) spectra. The spectra exhibit five peaks to indicate the presence of zinc, oxygen, magnesium, platinum, and tin in the film. The appearance of platinum is contributed from the platinum coating before SEM analysis to improve the conductivity while tin comes from the substrate. The presence of a relatively low intensity peaks for Mg compared to zinc and O peaks confirmed the success of Mg-doped into ZnO host. Furthermore, the EDS quantitative result depicted in Figure 2d) has shown that the concentration of Mg is about 1.32 %, which is slightly lower than the experimental design.



**Figure 2.** Scanning electron microscope images of Mg-doped ZnO with variations of annealing temperatures. (a) 400, (b) 500, (c) 550, and (d) representative EDS analysis

### 3.2. X-ray diffraction analysis

The crystal properties of Mg-doped ZnO were studied by X-ray diffraction technique. The results are shown in Figure 3. The X-ray diffraction patterns are similar to a wurtzite crystal structure based on the standard card of JCPDF #36-1451 (ZnO) [17]. It is also clearly seen that the intensity of X-ray diffraction increases as the temperature of annealing increased, which indicates an improvement in the crystallinity of Mg-Doped ZnO films with the rise in temperature.



**Figure 3.** X-ray diffraction pattern of Mg-doped ZnO thin films at different annealing temperatures.



The crystallite size of Mg-doped ZnO thin films at different annealing temperatures was then calculated with using Scherer equation [18].

$$D = \frac{0.9 \lambda}{\beta \cos \theta} \quad (3)$$

Where, D is the crystallite size (nm),  $\lambda$  is the wavelength (nm),  $\beta$  is the full half maximum (rad), and  $\theta$  is Bragg angle ( $^{\circ}$ ).

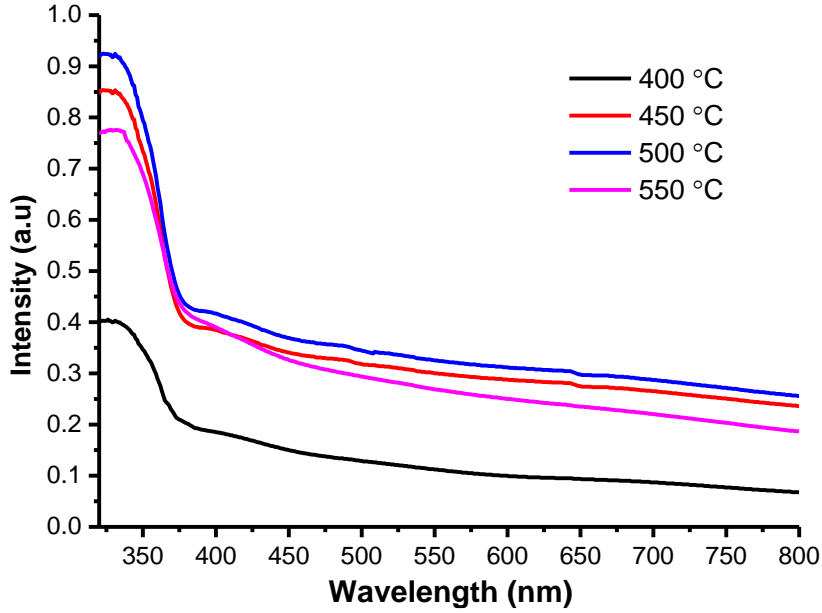
As listed in Table 1, the crystallite sizes do not clearly change for different annealing temperatures. All as-prepared Mg-doped ZnO thin films have the crystal size about 25 nm.

**Table 1.** Crystallite size of Mg-doped ZnO thin films at different annealing temperatures.

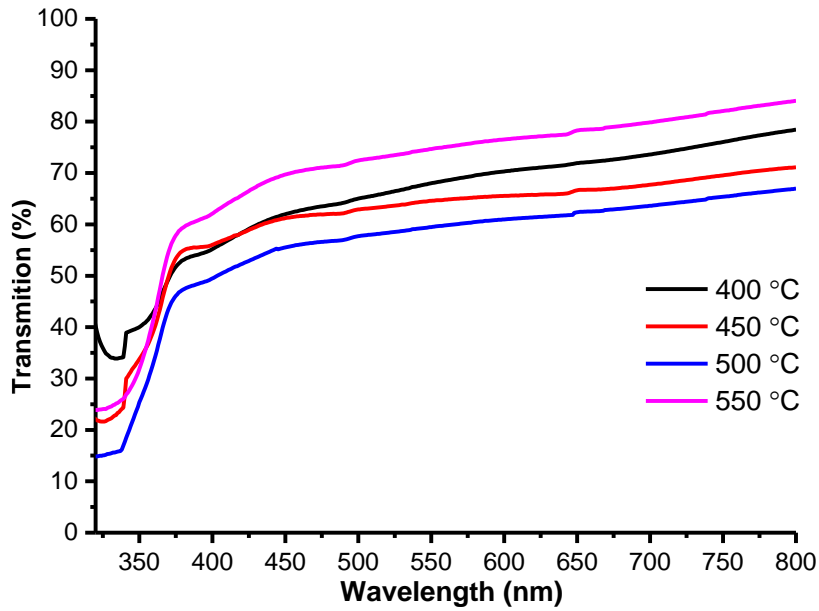
Temperature ( $^{\circ}$ C)	Crystallite size (nm)
400	25
450	24
500	24
550	25

### 3.2. Optical properties

To study the effect of different annealing temperatures on light absorption and transmission, spectra of as-prepared Mg-doped ZnO thin films were measured and the results were presented in Figure 4 and Figure 5, respectively. The absorption peaks of all Mg-doped ZnO thin films are located at a wavelength of 350 nm, which is the UV-region. As clearly shown in Figure 4, the absorption of Mg-doped ZnO annealed at 400 is quite low. However, after increasing the annealing temperature to 450  $^{\circ}$ C and 500  $^{\circ}$ C the absorption sharply elevates. Further, increasing the temperature of annealing to 550  $^{\circ}$ C leads to a lower absorbance but still higher than that at 400  $^{\circ}$ C. The transmission spectrum in Figure 5 also shows a similar trend to the absorption spectra in Figure 4. The thin films show transparency about 50-80 % at the visible light region.



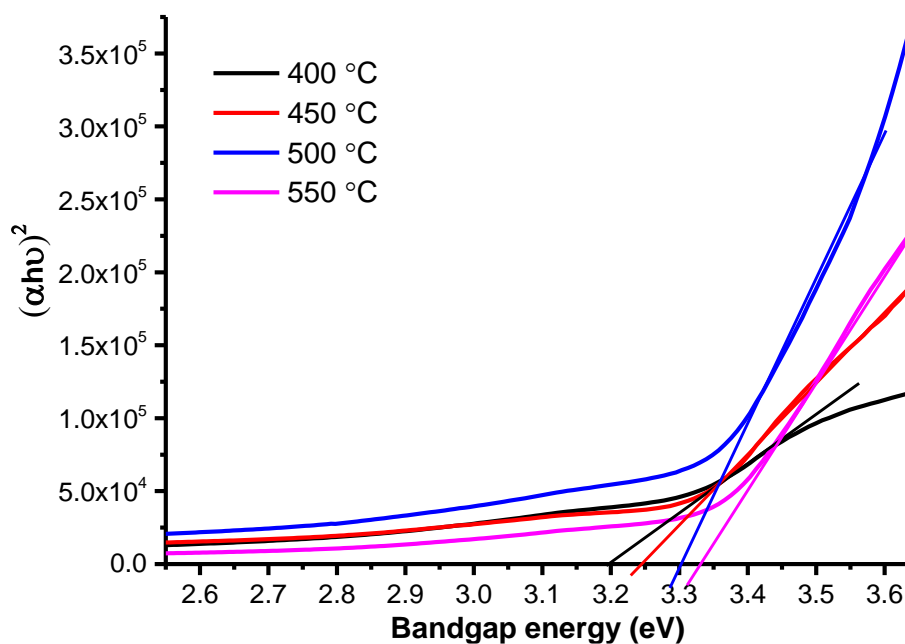
**Figure 4.** Absorption spectra of Mg-doped ZnO thin films at different annealing temperatures.



**Figure 5.** Transmittance spectra of Mg-doped ZnO thin films at different annealing temperatures.

The effect of different annealing temperatures on bandgap energies was studied using the Tauc plot, as presented in Figure 6. The bandgap values of Mg-doped ZnO thin films are 3.20, 3.24, 3.30, and 3.33 eV

for annealing at 400, 450, 500 and 550 °C respectively. The slight increment of bandgap energy with increasing temperature due to the increasing of grain size was also reported in the previous studies [19, 20].



**Figure 6.** Tauc plot of Mg-doped ZnO thin films at different annealing temperatures.

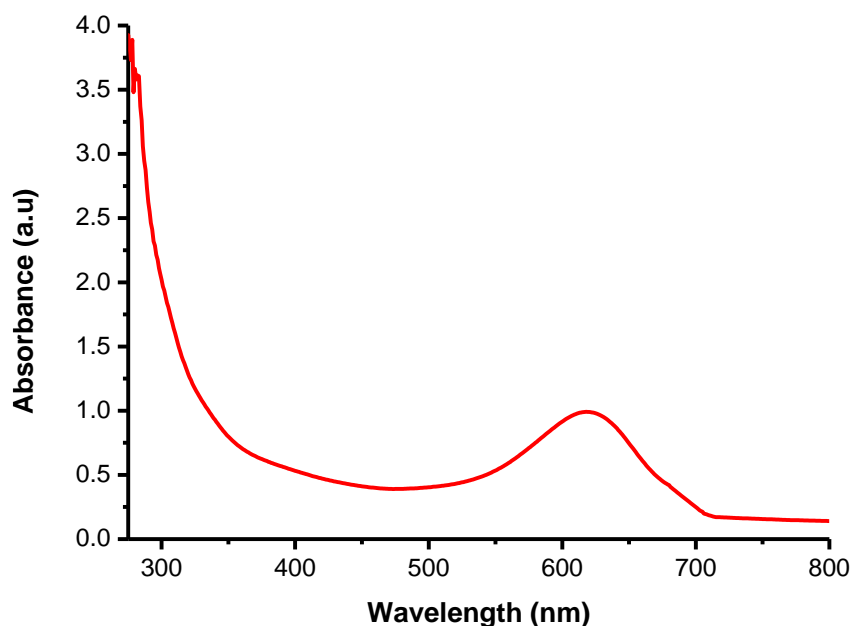
**Table 2.** Bandgap energy of Mg-doped ZnO thin film at different annealing temperatures.

Temperature (°C)	Energy bandgap (eV)
400 °C	3.20
450 °C	3.24
500 °C	3.30
550 °C	3.33

### 3.4. Absorbance of *Rhodomyrtus tomentosa* dye extract

The optical absorption spectrum of the extracted rose myrtle (*Rhodomyrtus tomentosa*) natural dye was measured using a UV-Vis spectrophotometer to investigate its sensitivity to light. As shown in Figure 7, the natural dye has a strong absorption at the visible-light region with an intense absorption peak at a

wavelength of 610 nm. This property is very useful for DSSC to improve the light absorption ability. It is also well known that 43% of the solar spectrum falls in the visible light range ; which is much more than 4% that irradiates in UV region [21]. The more light can be absorbed, more electron hole can be generated, which leads to a higher efficiency of a DSSC device.



**Figure 7.** Absorbance spectrum of natural dye of rose myrtle (*Rhodomyrtus tomentosa*).

### 3.5. Efficiency of DSSC

Table 3 lists the photovoltaic properties of DSSC fabricated from Mg-doped ZnO photoanode films (annealed at different temperatures) and the fruit extract of *Rhodomyrtus tomentosa* as a natural dye sensitizer. The efficiency of DSSC device annealed at 400 °C was about 1.66%. By increasing the temperature of annealing to 450 °C the efficiency also was increased to 2.36 %. Further increasing the temperature of annealing to 500 °C, the efficiency of 3.53 % can be achieved. However, the efficiency was observed to decline when the temperature of annealing is 550 °C. Therefore, the optimum temperature of annealing is 500 °C with a maximum of power conversion efficiency of 3.53%. Based on the

characterization result, the highest efficiency of 3.53% at 550 °C could be contributed to its highest degree of crystallinity (as indicated in the XDR spectra) and improved degree of conductivity of the photoanode thin films.

**Table 3.** Maximum voltage, current density, fill factor, and efficiency of DSSC for different annealing temperatures.

<b>Temperature (°C)</b>	<b>V<sub>max</sub> (V)</b>	<b>J<sub>max</sub> (mA/cm<sup>2</sup>)</b>	<b>P<sub>max</sub> (W/cm<sup>2</sup>)</b>	<b>P<sub>in</sub> (W/cm<sup>2</sup>)</b>	<b>FF (%)</b>	<b>η (%)</b>
400	0.5	0.15	0.61	36.5	81.0	1.66
450	0.5	0.12	0.86	36.5	146.8	2.36
500	0.5	0.20	1.29	36.5	127.4	3.53
550	0.5	0.78	0.68	36.5	174.2	1.85

#### 4. CONCLUSIONS

We have successfully fabricated a dye-sensitized solar cell (DSSC) device using Mg-doped ZnO thin film as the photoanode and natural dye of rose myrtle (*Rhodomyrtus tomentosa*) as the dye sensitizer. The electron microscope revealed that the surface of Mg-doped ZnO thin film was nanosphere. It is found that increasing the annealing temperature could lead to a larger grain size. The bandgap energy slightly increased by increasing the annealing temperature. The dye sensitizer had a strong absorption at the visible light region. The maximum efficiency of DSSC device was 3.53% with an annealing temperature of 500 °C. This work demonstrates that the annealing temperature of photoanode significantly affects the efficiency of DSSC device.

#### ACKNOWLEDGMENTS

The authors would like to thank the Rector of Universitas Negeri Medan for supporting this research.

#### REFERENCES

1. Gong, J., J. Liang, and K. Sumathy, *Review on dye-sensitized solar cells (DSSCs): Fundamental concepts and novel materials*. Renewable and Sustainable Energy Reviews, 2012. **16**(8): p. 5848-5860.
2. Wu, T.-L., et al., *Application of ZnO micro rods on the composite photo-electrode of dye sensitized solar cells*. Microsystem Technologies, 2018. **24**(1): p. 285-289.
3. Vittal, R. and K.-C. Ho, *Zinc oxide based dye-sensitized solar cells: A review*. Renewable and Sustainable Energy Reviews, 2017. **70**: p. 920-935.
4. Bekele, E.T., et al., *Biotemplated Synthesis of Titanium Oxide Nanoparticles in the Presence of Root Extract of *Kniphofia schemperi* and Its Application for Dye Sensitized Solar Cells*. International Journal of Photoenergy, 2021. **2021**: p. 6648325.
5. Mehmood, U., et al., *Recent Advances in Dye Sensitized Solar Cells*. Advances in Materials Science and Engineering, 2014. **2014**: p. 974782.
6. Roy, S., et al., *Enhanced performance of dye-sensitized solar cell with thermally stable natural dye-assisted TiO<sub>2</sub>/MnO<sub>2</sub> bilayer-assembled photoanode*. Materials for Renewable and Sustainable Energy, 2020. **9**.
7. Ye, M., et al., *Recent advances in dye-sensitized solar cells: from photoanodes, sensitizers and electrolytes to counter electrodes*. Materials Today, 2015. **18**(3): p. 155-162.
8. Sasidharan, S., et al., *Fine tuning of compact ZnO blocking layers for enhanced photovoltaic performance in ZnO based DSSCs: a detailed insight using  $\beta$  recombination, EIS, OCVD and IMVS techniques*. New Journal of Chemistry, 2017. **41**(3): p. 1007-1016.
9. Rashad, M., et al., *Physical and nuclear shielding properties of newly synthesized magnesium oxide and zinc oxide nanoparticles*. Nuclear Engineering and Technology, 2020. **52**(9): p. 2078-2084.

10. Fu, X., et al., *Large-Scale Growth of Ultrathin Low-Dimensional Perovskite Nanosheets for High-Detectivity Photodetectors*. ACS Applied Materials & Interfaces, 2020. **12**(2): p. 2884-2891.
11. Fang, D., et al., *Structural and optical properties of Mg-doped ZnO thin films prepared by a modified Pechini method*. Crystal Research and Technology, 2013. **48**(5): p. 265-272.
12. Jilani, A., M. Abdel-wahab, and A. Hammad, *Advance Deposition Techniques for Thin Film and Coating*. 2017.
13. Sengupta, J., A. Ahmed, and R. Labar, *Structural and optical properties of post annealed Mg doped ZnO thin films deposited by the sol-gel method*. Materials Letters, 2013. **109**: p. 265-268.
14. Mia, M.N.H., et al., *Influence of Mg content on tailoring optical bandgap of Mg-doped ZnO thin film prepared by sol-gel method*. Results in Physics, 2017. **7**: p. 2683-2691.
15. Arif, M., et al., *Effect of Annealing Temperature on Structural and Optical Properties of Sol-Gel-Derived ZnO Thin Films*. Journal of Electronic Materials, 2018. **47**(7): p. 3678-3684.
16. Chen, T.-H., et al., *Effects of different annealing temperature on the optoelectrical properties of MGZO thin films prepared by co-sputtering method*. Microsystem Technologies, 2019. **25**.
17. Gultom, N.S., H. Abdullah, and D.-H. Kuo, *Phase transformation of bimetal zinc nickel oxide to oxysulfide photocatalyst with its exceptional performance to evolve hydrogen*. Applied Catalysis B: Environmental, 2020. **272**: p. 118985.
18. Gultom, N.S., H. Abdullah, and D.-H. Kuo, *Facile synthesis of cobalt-doped (Zn,Ni)(O,S) as an efficient photocatalyst for hydrogen production*. Journal of the Energy Institute, 2019. **92**(5): p. 1428-1439.
19. Kasim, M.F., et al., *The Effect of Annealing Temperature on the Band Gap of ZnO Nano Materials*. Advanced Materials Research, 2012. **545**.

20. Sabeeh, S.H. and R.H. Jassam, *The effect of annealing temperature and Al dopant on characterization of ZnO thin films prepared by sol-gel method*. Results in Physics, 2018. **10**: p. 212-216.
21. Gultom, N.S., et al., *Transforming Zn(O,S) from UV to visible-light-driven catalyst with improved hydrogen production rate: Effect of indium and heterojunction*. Journal of Alloys and Compounds, 2021. **869**: p. 159316.



## Permintaan revisi tanggal 11 May 2021

4033692: Revision requested Inbox



**Carneiro Joaquim** <support@hindawi.com> [Unsubscribe](#)  
to me

Tue, May 11, 6:28 AM



Dear Siregar Nurdin,

In order for your submission "Fabrication of dye-sensitized solar cells (DSSC) using Mg-doped ZnO as photoanode and extract of rose myrtle (*Rhodomyrtus tomentosa*) as natural dye" to International Journal of Photoenergy to proceed to the review process, there needs to be a revision.

Reasons & Details:

“

*It is mandatory that the authors clearly answer all questions / suggestions (point by point) raised by the reviewers and make all corrections in accordance with the reviewers' report.*

For more information about what is required, please click the link below.

“

*It is mandatory that the authors clearly answer all questions / suggestions (point by point) raised by the reviewers and make all corrections in accordance with the reviewers' report.*

For more information about what is required, please click the link below.

[MANUSCRIPT DETAILS](#)

Kind regards,  
Carneiro Joaquim

International Journal of Photoenergy

This email was sent to [siregarnurdin@unimed.ac.id](mailto:siregarnurdin@unimed.ac.id). You have received this email in regards to the account creation, submission, or peer review process of a submitted paper, published by Hindawi Limited.

## — Reviewer Reports

3 submitted

## Report

Reviewer 4 09.05.2021

This study has some interesting results. The authors have done a good job and effort to comment on the results accordingly. However, the English of the presented study is below the expectations. Further, the presented study needs to be improved according to issues given below and the reason of the obtained findings need to be commended in more details with more supportive idea and references. Moreover, it will be a good advantage to state the aim of the presented investigation. Hence, after doing the issues and suggestions accordingly as given below, this study can be recommended for possible publication in the Journal.

1-There are many serious mistakes in the English grammar and writing rules (some of them are denoted in the attached file). Therefore, it is suggested to review and check the manuscript by the English grammar expertise to correct it carefully.

2- The authors have expressed that the SEM images reveal that the surface of Mg-doped ZnO thin film is nanosphere (introduction and page 5). This statement is physically not meaningful. It will be much meaningful if they state as the SEM images reveal that the grain/particle shape of the surface of the Mg-doped ZnO thin film is nanosphere. Similarly, the success of Mg-doped into ZnO host (the successful Mg doping into ZnO host)

3-It will be useful to enlarge the introduction according to the followings, recommended to mention them within the text, in terms of advantage and physical/chemical characterizations of the sol-gel technique and ZnO semiconductor: (i) Journal of Alloys and Compounds, 158734, 2021; (ii) Brazilian Journal of Physics volume 51, pages544–552(2021); (iii) Applied Physics A 126 (10), 2020, 1-6.

4-Please do not start with a bigger uppercase letter (Sol-gel spin page 3) except for the after the dot. If you use any abbreviation (like XRD) please do not use the main word like x-ray diffraction. Also please do not use the united words/items like and4

5-The authors have stated that it is also clearly seen that the intensity of X-ray diffraction increases as the temperature of annealing increased, which indicates an improvement in the crystallinity of Mg-Doped ZnO films with the rise in temperature (i) and the crystallite sizes do not clearly change for different annealing temperatures. (ii). these two statements do not agree with each other.

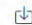
6- Please add or calculate peak intensity, diffraction angles, lattice parameters, micro-strain, and dislocation density of all samples. And also discuss their influences on the measured or presented properties. For the calculation and comments, it is suggested to use the followings, which will be a good advantage to mention them within the text. (i) Thin Solid Films 680, 2019, 20-30 (ii) Sensors 2021, 21(6), 2110; (iii) Materials Research Express 6 (3), 2019, 035903; (iv) Thin Solid Films, 717, 2021, 138447.

7- The followings are contradicted please correct them; (i) Therefore, the optimum temperature of annealing is 500 oC with a maximum of power conversion efficiency of 3.53%; (ii) Based on the characterization result, the highest efficiency of 3.53% at 550 oC could be contributed to its highest degree of crystallinity.

8-The explanations/reasons for the variation in transmittance, absorbance, and bandgap widening by annealing temperatures need to be addressed with more details. Also, discuss about the relationship between the lattice parameters and the bandgap of the produced film samples. It is suggested to use the following for references, which will help you to explain the issue: (i) Materials Science in Semiconductor Processing 75, 221-233; (ii) Optical Mater. 114, 2021, 110908; (iii) Journal of Sol-Gel Science and Technology 90 (3), 487-497.

8-The explanations/reasons for the variation in transmittance, absorbance, and bandgap widening by annealing temperatures need to be addressed with more details. Also, discuss about the relationship between the lattice parameters and the bandgap of the produced film samples. It is suggested to use the following for references, which will help you to explain the issue: (i) Materials Science in Semiconductor Processing 75, 221-233; (ii) Optical Mater. 114, 2021, 110908; (iii) Journal of Sol-Gel Science and Technology 90 (3), 487-497.

**File**

Spelling mistakes in manuscript.docx 4 MB 

**Report**

Reviewer 3 05.05.2021

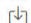
1. Abstract: There is a confusion by authors between crystallite/grain size vs particles size.
2. P5: The particles have irregular shapes instead of nanospheres shapes.
3. P5: It is more appropriate to use the term "particle size" instead of "grain size" as the FESEM images would not be able to indicate that the particle only contained single grain or polygrains.
4. P6: It is good to have FESEM images for samples without annealing (as-deposited) and annealed at 450 oC in Figure 2 for comparison purpose.
5. P6: The present of Mg element in the EDS analysis does not mean that Mg has been successfully doped into the ZnO and they are electrically active. More evident are needed to prove that Mg has been doped into the ZnO particles.
6. P7: Please index the diffraction planes in the XRD results as shown in Figure 3.
7. P7: It is good to include the XRD of as-deposited thin film in Figure 3 for comparison purpose.
8. P8: Why lower absorbance was obtained when the annealing temperature was 550 oC as shown in Figure 4?
9. P9: Why the transmittances (not "transmission") of Mg-doped ZnO thin films annealed at different temperature were random?
10. P10: Why increase of particle size (not "grain size") will caused increment in bandgap energy?
11. P12: The highest efficiency of 3.53 % was achieved using ZnO thin film annealed at 500 oC (not 550 oC). Thus, the claim of improved degree of conductivity in this context is not correct.
12. Suggest to highlight the problem(s) to be addressed in this paper in introduction. Also, to highlight the novelty of this work.

**Report**

Reviewer 1 11.05.2021

This contribution reports interesting results on a ZnO-Mg based DSSC using a natural extract as photosensitizer. Yet the manuscript has serious flaws such as fill factors above 100% and the presented data does not entirely support the given conclusions. Also the english writing is very poor. I attach an annotated pdf file of the manuscript with all my comments/corrections that must be addressed before the contribution is suitable for publication. The pdf file was created using MS-Word and annotated using Okular software running under linux/KDE. I was almost rejecting this work but decided to give it a second chance.

**File**

Manuscript\_Hindawi-commented.pdf 1 MB 

Submitted revisi ke -1 tanggal 11 may 2021



Nurdin

← BACK DASHBOARD / ARTICLE DETAILS

Updated on 2021-05-11 Version 2

## Fabrication of dye-sensitized solar cells (DSSC) using Mg-doped ZnO as photoanode and extract of rose myrtle (*Rhodomyrtus tomentosa*) as natural dye

[VIEWING AN OLDER VERSION](#)

ID 4033692

Nurdin Siregar <sup>SA</sup> <sup>CA</sup> <sup>1</sup>, Motlan Motlan<sup>1</sup>, Jonny Haratua Panggabean<sup>1</sup>, Makmur Sirait<sup>1</sup>, Juniastel Rajaguguk<sup>1</sup>, Noto Susanto Gultom<sup>1</sup>, Fedlu Kedir Sabir<sup>2</sup> + [Show Affiliations](#)

### Article Type

Research Article

### Journal

International Journal of Photoenergy

Chief Editor [Giulia Grancini](#)

Academic Editor [Carneiro Joaquim](#)

Submitted on 2021-05-11 (5 months ago)

> Abstract

> Author Declaration

▼ Files 3

#### Main manuscript

Manuscript\_clean.docx

4 MB



#### Cover letter

Cover letter\_revised.docx

14 kB



#### Supplemental files

Manuscript\_markup editing.docx

5 MB



## Fabrication of dye-sensitized solar cells (DSSC) using Mg-doped ZnO as photoanode and extract of rose myrtle (*Rhodomyrtus tomentosa*) as natural dye

Nurdin Siregar<sup>1\*</sup>, Motlan<sup>1</sup>, Jonny Haratua Panggabean<sup>1</sup>, Makmur Sirait<sup>1</sup>, Juniastel Rajagukguk<sup>1</sup>, Noto Susanto Gultom<sup>1</sup>, Fedlu Kediri Sabir<sup>2</sup>.

<sup>1</sup>Department of Physics, Faculty of Mathematics and Natural Sciences, State University of Medan, Jl. Willem Iskandar Pasar Medan Estate, Medan 20221, Indonesia

<sup>2</sup>Department of Applied Chemistry, School of Applied Natural Science, Adama Science and Technology University, P.O. Box 1888, Adama, Ethiopia

\*Corresponding author: [siregarnurdin@unimed.ac.id](mailto:siregarnurdin@unimed.ac.id)

### ABSTRACT

A dye-sensitized solar cell (DSSC) device using Mg-doped Zn thin films as photoanode and fruit extract of rose myrtle (*Rhodomyrtus tomentosa*) as the natural dye was investigated. The effect of annealing temperature (400-550 °C) on the films of photoanode was systematically studied using an X-ray diffractometer (XRD), UV-Visible Near Infrared (UV-Vis NIR) Spectrophotometer, scanning electron microscopy (SEM), and energy dispersive spectroscopy (EDS). XRD confirm that all sample has the wurtzite hexagonal with crystallite size of 25 nm. The SEM images reveal that particles of the surface of the Mg-doped ZnO thin film are irregular shapes ~~the surface of Mg-doped ZnO thin film is nanosphere~~. Increasing the annealing temperature leads to a larger grain-particle size and slightly increases bandgap energy. The dye sensitizer of extracted rose myrtle (*Rhodomyrtus tomentosa*) has a strong absorption at the visible light region. The maximum efficiency of the DSSC device is 3.53% with Mg-ZnO photoanode annealed at 500 °C.

**Keywords:** Dye Sensitized Solar Cell, Mg-doped ZnO, sol-gel spin coating, natural dye

## 1. INTRODUCTION

The ~~higher~~ demands ~~of for~~ renewable energy continually increase every ~~\_single\_~~ year due to its eco-friendliness ~~and regenerality~~. Solar cells have been well known as a device to convert solar energy to electricity for decades. However, the conventional solar cells are still ~~competitive in the~~ high price market ~~with due to~~ complicated fabrication process and expensive of raw materials. Dye-sensitized solar cell (DSSC), is one of the most promising solar cell types to ~~generate produce~~ renewable energy with a low-cost material and simple fabrication process [1-3]. The working principal of DSSCs is the utilized during the solar irradiation to convert into electric current. After irradiation, the dye sensitizer harvests light and causes an electron to promote the conduction band leaving a hole in the valence band. There are numerous pigments of plant leaves, fruits, and flowers that have the potential to be utilized in DSSC. The variety of pigments with different ~~width of light harvesting wavelenghts ranges~~ and degrees of absorptivity in UV-Visible spectrum can cause different performances of DSSC. The molecules of the dye can be anchored into the surface areas of the semiconductor to form Lewis acid-base types of interaction to enhance electron transfer from HOMO of the dye molecule (pigment) to the conduction band of the semiconductor (anode) [4-7].

Zinc oxide (ZnO) semiconductor plays an important role as a photoanode to improve the conducting interface layer and to enhance the power conversion efficiency (PCE). According to the literatures, ZnO has a high electron mobility, wide bandgap (3.37eV), and large exciton binding energy of 60 meV [8]. Magnesium (Mg) is one of the metals that is used in many applications such as refractory materials, optical and heating apparatus [9, 10]. ~~This material~~ Mg-doped ZnO material also has special properties to block the electron due to of its wide bandgap [11, 12]. There are several methods to grow thin film on a substrate, such as molecular beam epitaxy, metal organic chemical vapor deposition, plasma

Formatted: Highlight

enhanced chemical deposition, sputtering method, spray pyrolysis, atomic layer deposition, pulse laser deposition, electron beam evaporation, and sol-gel [13]. The sol-gel method has several advantages compared to aforementioned methods such as simple, cheap, and efficient [14-16]. By using a sol-gel spin coating technique, several parameters like concentration of precursor solution, annealing ~~temperature~~~~temperature~~, annealing time, and so on can be easily tuned in order to achieve the desired properties [12, 17].

In this work, the photoanodes of Mg-doped ZnO thin films were prepared by a ~~s~~Sol-gel spin coating method. To the best of our knowledge, the ~~natural dye~~ from the fruit extract of *Rhodomyrtus tomentosa* has not been reported yet as the dye sensitizer for DSSC. The effect of different annealing temperatures on structural and optical properties of Mg-doped ZnO photoanodes as well as the efficiency of DSSC device was systematically investigated using necessary characterization tools. We find that the maximum efficiency of the DSSC device is 3.53% with Mg-doped ZnO photoanode annealed at 500 °C.

## 2. EXPERIMENTAL SECTION

### 2.1. Synthesis of Mg-doped ZnO thin films

Mg-doped ZnO thin films were fabricated using a sol-gel spin coating technique. Typically, zinc Acetate dehydrate and magnesium chloride (2 ~~wt.~~%) were dissolved in isopropanol (35 mL) under continuous stirring. After 10 min, 1.7 mL diethanolamine was added slowly into the solution. After refluxing process at 90 °C for about 2 hours, the gel was dropped on top of FTO glass and spun at 5000 rpm for 60 s. After the drying process, the samples were ~~annealed~~ annealed at different temperatures of 400, 450, 500, and 550°C for 5 hours.

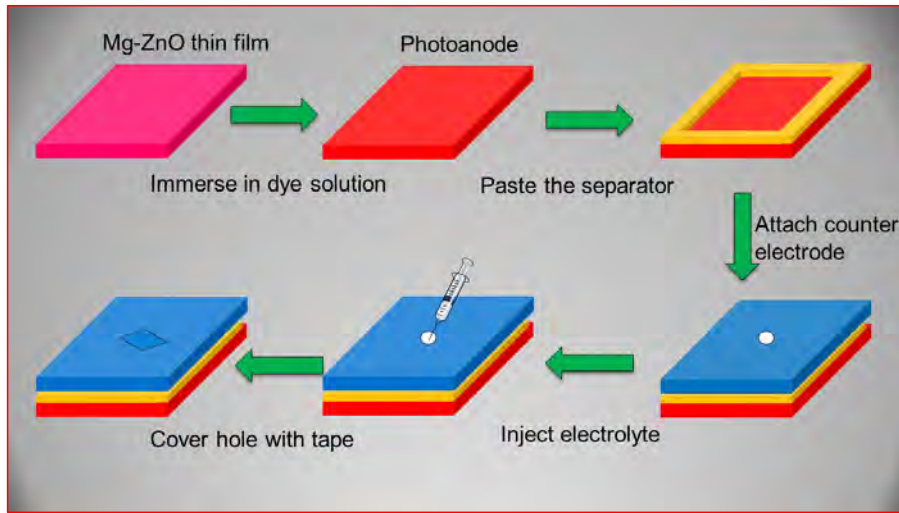
### 2.2. Extraction of natural dyes



About 50 grams of *Rhodomyrtus tomentosa* fruit was ground using a mortar. After being moved into a beaker glass, 25 mL DI water, 21 mL ethanol, and 4 mL acetic acid were added and then stirred to form a ~~homogeneous~~ homogenous solution. The solution was then covered with aluminum foil to avoid photooxidation and soaked at room temperature for 24 h. Finally, the solid and liquid parts were separated using filter paper. The filtered solution of *Rhodomyrtus tomentosa* fruit extract was ready to be used as the sensitizer in DSSCs.

### 2.3. Fabrication of DSSC

Figure 1 illustrates the schematic fabrication of the DSSC device. First, the as-prepared Mg-doped ZnO thin film was used as the photoanode electrode. Natural-dye sensitized from *Rhodomyrtus tomentosa* fruit extract was adsorbed on the top of Mg-doped ZnO photoanode by immersing it into the extracted dye solution for several hours. After that, it was taken out and washed with ethanol to remove the unadsorbed dye and dried in the oven at 80 °C. The platinum coated on the glass FTO was used as the counter electrode. The DSSCs were assembled by attaching the photoanode and the counter electrode using thermoplastic sealant surlyn as glue and separator. And then heated at 80 °C to let the surlyn perfectly attach to the electrodes. The electrolyte was injected through a tiny hole on that was drilled on the counter electrode. Finally, that hole was covered with transparent tape.



**Figure 1.** Schematic of the fabrication of DSSC using Mg-doped ZnO photoanode and fruit extract of *Rhodomyrtus tomentosa*.

Formatted: Indent: First line: 0"

#### 2.4. Characterization tools

To observe the surface morphology of Mg-doped ZnO thin films annealed at different temperatures, a scanning electron microscope (JEOL-6500) analysis was performed at an accelerating voltage of 15 kV. The X-ray diffraction (XRD) [pattern](#) of Mg-doped ZnO thin films were analyzed using an X-ray diffractometer (LabX XRD-6100, Shimadzu) with Cu K $\alpha$  ( $\lambda=1.54 \text{ \AA}$ ). The transmittance and absorbance spectra were recorded using a UV-Vis NIR spectrophotometer. The efficiency of the DSSC was measured using an I-V measurement (Keitly Source Measure Unit) system by irradiating a photoanode electrode with a LED and input power of [35 mW/cm<sup>2</sup>-light source](#). Several data such as open-circuit voltage ( $V_{oc}$ ), short circuit current density ( $J_{sc}$ ), maximum voltage ( $V_{max}$ ), and maximum current ( $J_{max}$ ) were recorded. Then, the fill factor (FF) and efficiency ( $\eta$ ) were determined using equations (1) and (2), respectively.

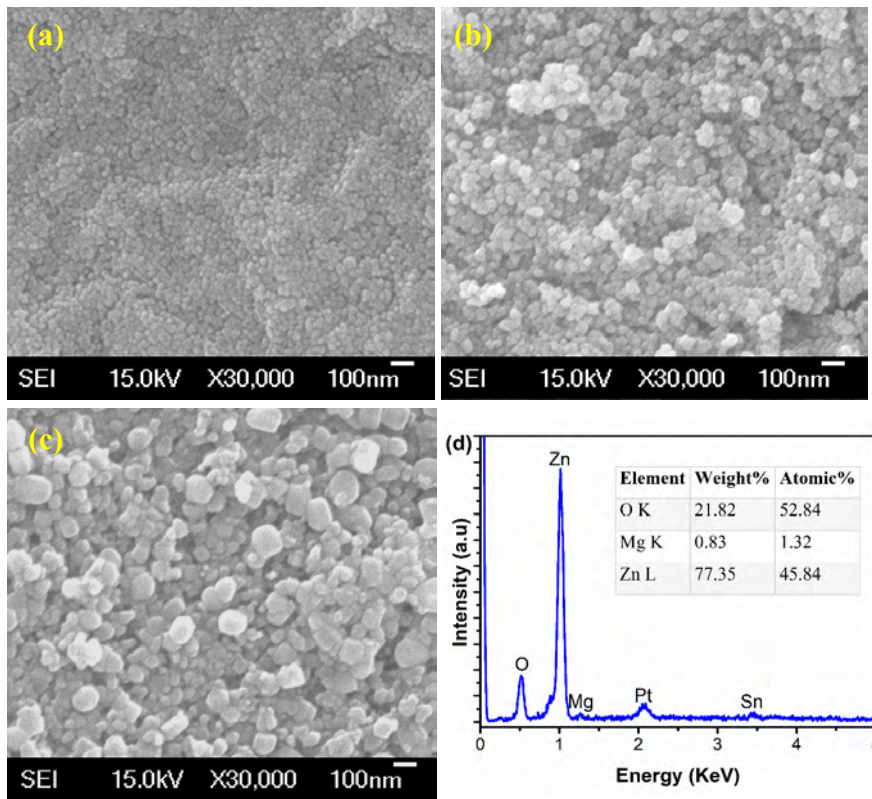
$$FF = \frac{J_{max} \times V_{max}}{J_{sc} \times V_{oc}} \quad (1)$$

$$\eta = FF \frac{J_{sc} \times V_{oc}}{P_{in}} \times 100\% \quad (2)$$

### 3. RESULTS AND DISCUSSION

#### 3. 1. *Electron microscope analysis*

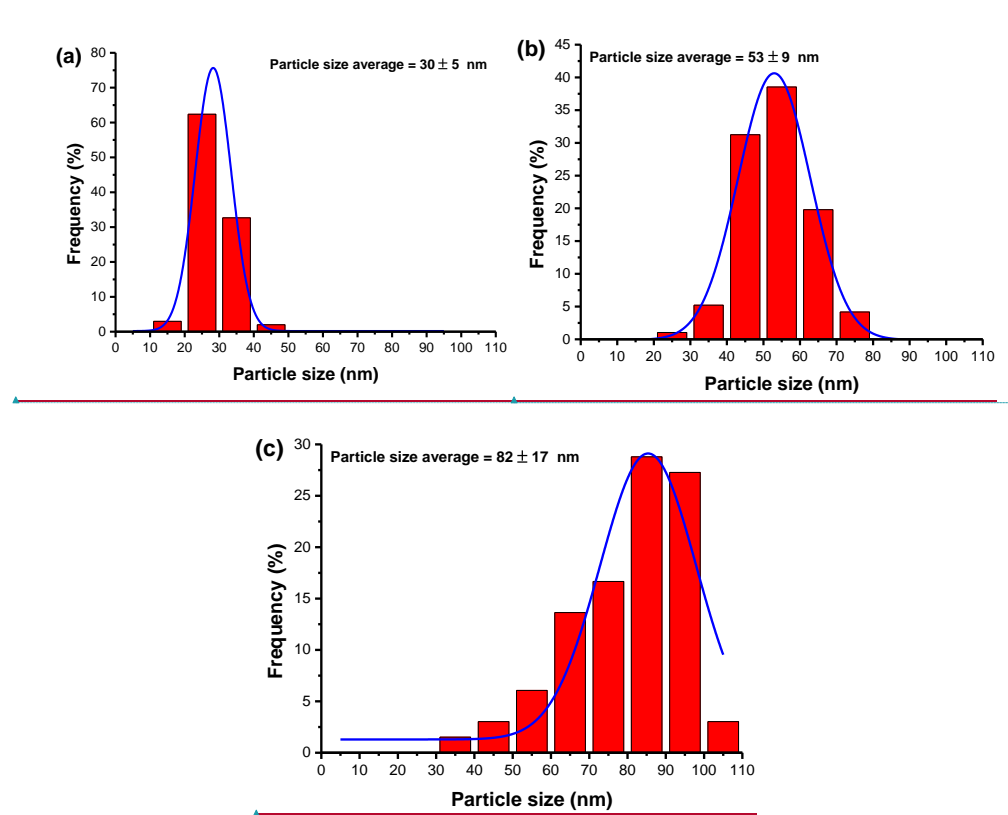
The surface morphology of Mg-doped ZnO with variation of ~~annealing~~ annealing temperatures was investigated using a field-emission scanning electron microscope. With a magnification of 30 k times, the top view images of Mg-doped ZnO thin films can be clearly observed in Figure 2. The surface microstructure of Mg-doped ZnO at different annealing temperatures ~~looks similar to~~ shows ~~nanosphere~~ nanoparticles with irregular shapes. It was clearly observed that by increasing the annealing temperature, the ~~grain-particle~~ size was monotonically increased. Figure 2d shows the representative energy dispersive spectroscopy (EDS) spectra. The spectra exhibit five peaks to indicate the presence of zinc, oxygen, magnesium, platinum, and tin in the film. The appearance of platinum is contributed from the platinum coating before SEM analysis to improve the conductivity while tin comes from the substrate. The presence of a relatively low intensity peak for Mg compared to zinc and O peaks confirmed the successful Mg doping into ZnO host. Furthermore, the EDS quantitative result depicted in Figure 2d has shown that the weight and atomic percentage of Mg are about 0.83 and 1.32 %, respectively.



**Figure 2.** Scanning electron microscope images of Mg-doped ZnO with variation of annealing temperatures. (a) 400, (b) 500, (c) 550, and (d) representative EDS analysis

To calculate the grain-particle size more precisely, further analysis was conducted using J-image-J analysis. As shown in Figure 3, the average particle sizes for Mg-doped ZnO thin films annealed at 400, 500, and 550 °C are  $30 \pm 5$ ,  $53 \pm 9$ , and  $82 \pm 17$  nm, respectively. A larger particle size at a higher annealing temperature was reasonable. It could be explained due to a higher driving force from thermal

energy that leads to a faster particle growth through Ostwald ripening mechanism. Our findings also well agree with some previous reports [18, 19].

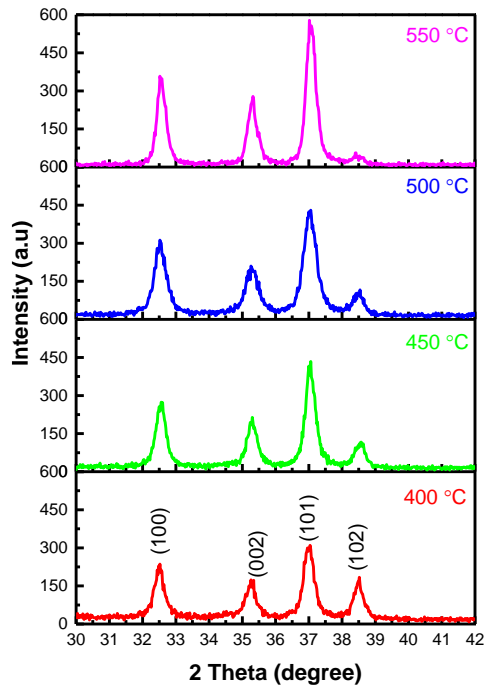


**Figure 3.** Particle size distribution of Mg-doped ZnO annealed at (a) 400, (b) 500, and (c) 550 °C

### 3.2. X-ray diffraction (XRD) analyses

The crystal properties of Mg-doped ZnO were studied by X-ray diffraction (XRD) technique. The results are shown in Figure 4. The XRD patterns are similar to a wurtzite crystal structure based on the standard card of JCPDF #36-1451 (ZnO) [20]. The intensity of peaks in Figure 4 gradually elevates as the

temperature of annealing increase, which indicates an improvement in the crystallinity of Mg-Doped ZnO films.



**Figure 34.** XRD pattern of Mg-doped ZnO thin films at different annealing temperatures.

Table 1 lists the summary of structural properties of Mg-doped ZnO thin films at different annealing temperatures. The average ~~crystallite~~ crystallite size of Mg-doped ZnO thin films was calculated at (101) plane using Scherer formula as shown in equation (3) [21]. Their crystallite size values are 20.60, 21.23, 16.83, and 22.9 nm at the annealing temperature of 400, 450, 500, and 550 °C, respectively. Next, ~~the~~ dislocation density ( $\delta$ ) of Mg-doped ZnO was further determined by equation (4) [22]. The dislocation density of Mg-doped ZnO annealed at 400, 450, 500 and 550 °C are  $2.36 \times 10^{-3}$ ,  $2.22 \times 10^{-3}$ ,  $3.53 \times 10^{-3}$ , and  $1.89 \times 10^{-3} \text{ nm}^{-2}$ , respectively. Mg-doped ZnO annealed at 500 °C has the highest dislocation density

Formatted: Superscript

Formatted: Superscript

Formatted: Superscript

Formatted: Superscript

Formatted: Superscript

compared to other samples. Macrostrain value that indicates the peak shift position was calculated according to equation (5) [23]. Based on the database, the (101) plane for ZnO located at 36.25 ° with an interplanar spacing of 2.4759 Å. However, the (101) plane for our Mg-doped ZnO is found at about 37.00 ° for 2θ with a calculated interplanar spacing of 2.4272 Å. The peak shifting of about 0.75 ° for 2θ also indicates that Mg as a dopant has been successfully doped into ZnO host lattice [24]. The macrostrain value was similar for different temperatures with a value of  $1.97 \times 10^{-2}$  because of their similarity in peak position. Based on the previous reports [25, 26], the lattice parameters *a* and *c* of Mg-doped ZnO were estimated to be about 3.172 Å and 5.080 Å using equations (6) and (7), respectively. The lattice parameter *a* at (100) plane did not significantly different for different annealing temperatures because their peak position was located almost in the same diffraction angle. Similarly, the lattice parameter *c* at (002) plane also very similar at different annealing temperatures, as listed in Table 1.

$$D = \frac{0.9 \lambda}{\beta \cos \theta} \quad (3)$$

Where, *D* is the ~~crystallite~~crystallite size (nm),  $\lambda$  is the wavelength (nm),  $\beta$  is the full half maximum, FWHM (rad), and  $\theta$  is Bragg angle (°).

$$\delta = \frac{1}{d^2} \quad (4)$$

$$\langle e \rangle = \frac{d - d_0}{d_0} \quad (5)$$

Where,  $d_0$  is the interplanar spacing of pure ZnO without deformation while  $d$  is the calculated interplanar spacing for Mg-doped ZnO at (101) plane using Bragg law.

$$a = \frac{\lambda}{\sqrt{3} \sin \theta_{(100)}} \quad (6)$$

$$c = \frac{\lambda}{\sin \theta_{(002)}} \quad (7)$$

Formatted: Superscript

Formatted: Font: Italic

Formatted: Font: Italic

**Table 1.** Summary of crystal properties of FWHM, Crystallite size, dislocation density, macrostrain values, and lattice parameters ( $a$  and  $c$ ) of Mg-doped ZnO thin films at different annealing temperatures.

Temperature (°C)	FWHM/ $\beta$ (rad)	Crystallite size (nm)	Dislocation density $\times 10^{-3}$ (nm <sup>-2</sup> )	Macro strain values $\langle e \rangle$	Lattice parameters (Å)	
					$a$	$c$
400	0.4065	20.6025	2.36	$1.97 \times 10^{-2}$	3.176	5.082
450	0.3945	21.2324	2.22	$1.97 \times 10^{-2}$	3.172	5.080
500	0.4976	16.8324	3.53	$1.97 \times 10^{-2}$	3.175	5.083
550	0.3645	22.925	1.89	$1.97 \times 10^{-2}$	3.173	5.080

### 3.2. Optical properties

To study the effect of different annealing temperatures on optical properties, the absorption and transmission spectra of Mg-doped ZnO thin films were measured and presented in Figure 54 and Figure 56, respectively. The absorption peaks of all Mg-doped ZnO thin films are located at a wavelength of 350 nm, which is at the UV region. As clearly shown in Figure 54, the absorption of Mg-doped ZnO annealed at 400 is quite low. However, after increasing the annealing temperature to 450 °C and 500 °C the absorption sharply elevates. Further, increasing the temperature of annealing to 550 °C leads to a lower absorbance but still higher than that at 400 °C. The transmission spectrum in Figure 65 exhibits transmission spectra of Mg-doped ZnO which also shows a similar trend to the absorption spectra in Figure 54. The thin films have show transparency about 50-80 % at the visible light region.

- Formatted: Font: Not Bold
- Formatted: Font: Not Bold
- Formatted: Justified, Space After: 8 pt, Line spacing: 1.5 lines
- Formatted: Font: Not Bold
- Formatted: Font: Italic
- Formatted: Font: Italic
- Formatted: Superscript
- Formatted: Superscript
- Formatted: Font: Italic
- Formatted: Font: Italic, English (United States)
- Formatted: Font: Italic
- Formatted: Font: Italic, English (United States)
- Formatted: English (United States)
- Formatted: English (United States)
- Formatted: Superscript
- Formatted: English (United States)
- Formatted: Superscript
- Formatted: English (United States)
- Formatted: English (United States)
- Formatted: English (United States)
- Formatted: English (United States)
- Formatted: English (United States)
- Formatted: Superscript
- Formatted: English (United States)
- Formatted: English (United States)
- Formatted: English (United States)



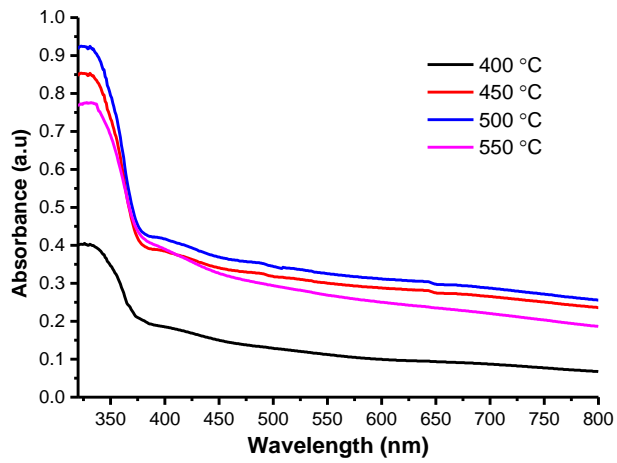
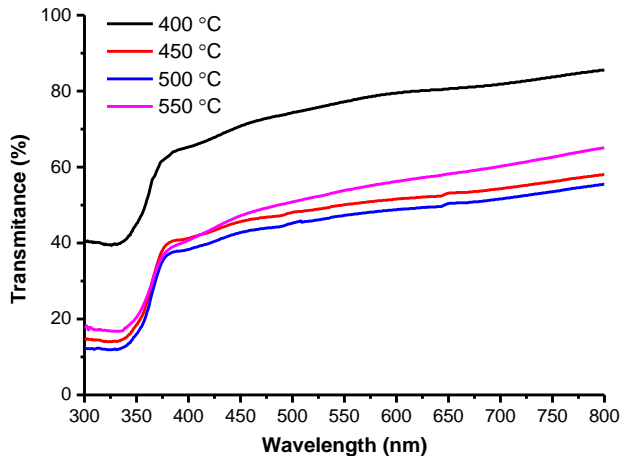
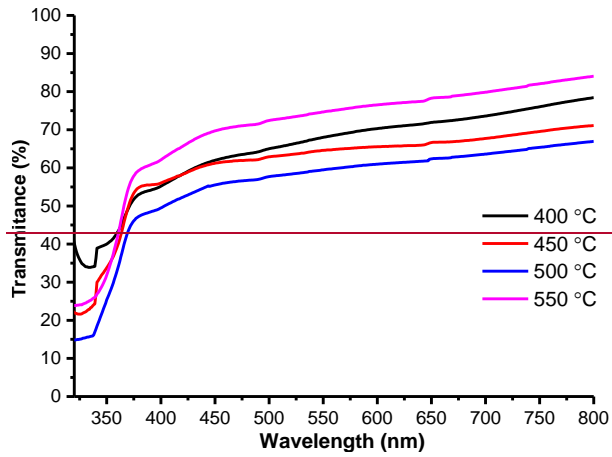


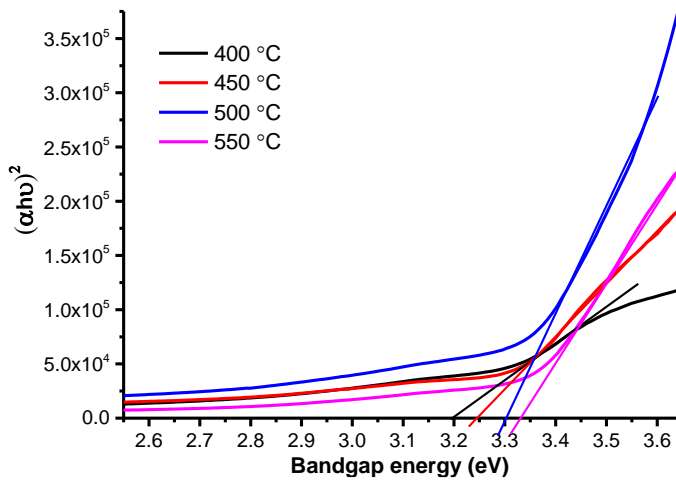
Figure 54. Absorbance spectra of Mg-doped ZnO thin films at different annealing temperatures.



Field Code Changed

**Figure 56.** ~~Transmittance~~ ~~Transmission~~ ~~spectrums~~ of Mg-doped ZnO thin films at different annealing temperatures.

The bandgap energy of Mg-doped ZnO thin films was further derived based on the optical absorption data and plotted in Figure 7. As listed in Table in 2, bandgap energy values are 3.20, 3.24, 3.30, and 3.33 eV for annealing at 400, 450, 500, and 550 °C respectively. The slight increment of bandgap energy with increasing temperature might be due to the Burstein–Moss effect as reported in previous studies [25, 27].



**Figure 76.** Tauc plot of Mg-doped ZnO thin films at different annealing temperatures.

**Table 2.** Bandgap energy of Mg-doped ZnO thin film at different annealing temperatures.

Temperature (°C)	Bandgap energy (eV)
400 °C	3.20
450 °C	3.24
500 °C	3.30
550 °C	3.33

Formatted Table

### 3.4. Absorbance of *Rhodomyrtus tomentosa* dye extract

The optical absorption spectrum of the extracted rose myrtle (*Rhodomyrtus tomentosa*) natural dye was measured using a UV-Vis spectrophotometer to investigate its sensitivity to light. As shown in Figure 87, the natural dye has a strong absorption at the visible-light region with an intense absorbance peak at a wavelength of 610 nm. This property is very useful for DSSC to improve the light absorption ability. It is also well known that about 43% of the solar spectrum falls in the visible light range; which is much more than and only 4% is that irradiates in the UV region [28]. The more light can be absorbed, the more electron-hole can be generated, which leads to a higher efficiency of a DSSC device.

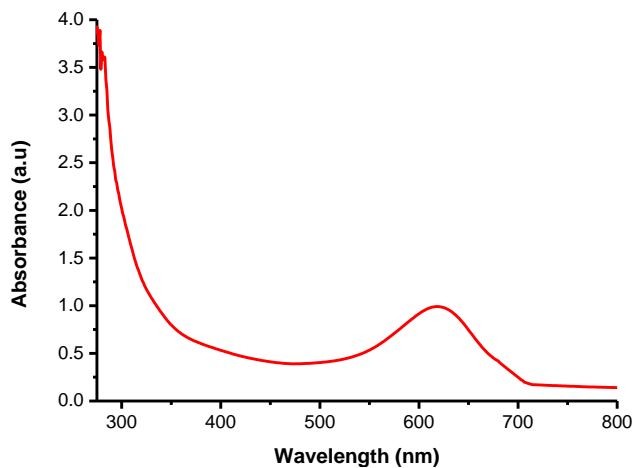
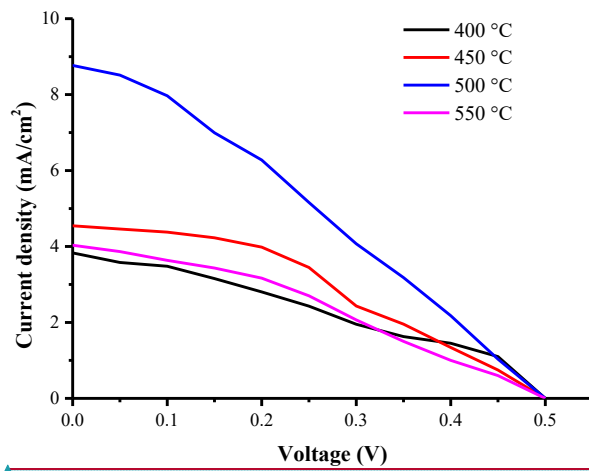


Figure 78. Absorbance spectrum of natural dye of extracted rose myrtle (*Rhodomyrtus tomentosa*).

### 3.5. Efficiency of DSSC

Figure 9 exhibits the *J-V* characteristic curve of DSSC with Mg-doped ZnO as photoanode at different annealing temperatures and the fruit extract of *Rhodomyrtus tomentosa* as a natural dye sensitizer. Further, the photovoltaic properties of DSSC are listed in Table 3. The open-circuit voltage ( $V_{oc}$ ) at different annealing temperatures was similar with a value of 0.5 V. In contrast, the short-circuit current ( $J_{sc}$ ) was significantly different. The  $J_{sc}$  values are 3.83, 4.55, 8.77, and 4.03 mA/cm<sup>2</sup> at annealing temperatures of

400, 450, 500, and 550 °C, respectively. The efficiency of the DSSC device annealed at 400 °C was about 1.66%. By increasing the annealing temperature to 450 °C the efficiency also was increased to 2.36 %. Further increasing the annealing temperature to 500 °C, the efficiency of 3.53 % can be achieved. However, the efficiency was observed to decline when the annealing temperature is 550 °C. Therefore, the optimum annealing temperature is 500 °C with a maximum power conversion efficiency of 3.53%. Based on the characterization results, the highest efficiency of 3.53% at 500 °C could be contributed due to its highest degree of optical absorption (as indicated in therevealed by UV-Vis analysis in Figure 5\_spectra) and improved degree of conductivity of the photoanode thin films.



**Figure 9.** J-V characteristic curve of DSSC using Mg-doped ZnO as photoanode at different annealing temperatures.

**Table 3.** Summary of electrical properties including  $V_{ocmax}$ , open-circuit voltage, short-circuit current, fill factor, and efficiency of DSSC for different annealing temperatures.

Temperature (°C)	$V_{ocmax}$ (V)	$J_{scmax}$ (mA/cm <sup>2</sup> )	$P_{max}$ (mW/cm <sup>2</sup> )	FF (%)	$\eta$ (%)
---------------------	--------------------	--------------------------------------	------------------------------------	-----------	---------------

Field Code Changed

Formatted: Centered

400	0.5	<del>3.830.15</del>	0.61	<del>81.031.70</del> <del>37.93+46.</del>	1.66
450	0.5	<del>4.550.12</del>	0.86	<del>8</del> <del>29.42+27.</del>	2.36
500	0.5	<del>8.770.20</del>	1.29	<del>4</del> <del>33.47+74.</del>	3.53
550	0.5	<del>4.030.78</del>	0.68	<del>2</del>	1.85

#### 4. CONCLUSIONS

We have successfully fabricated a dye-sensitized solar cell (DSSC) device using Mg-doped ZnO thin film as the photoanode and natural dye of rose myrtle (*Rhodomyrtus tomentosa*) as the dye sensitizer. The scanning electron microscope analysis revealed that the surface of Mg-doped ZnO thin film was ~~nanosphere particles with irregular shapes~~. It is found that increasing the annealing temperature led to a larger ~~grain particle~~ size and slightly increased bandgap energy. The natural rose myrtle dye sensitizer had a strong absorption at the visible light region. The maximum efficiency of the DSSC device was 3.53% at an annealing temperature of 500 °C. This work demonstrates that the annealing temperature of photoanode significantly affects the efficiency of the DSSC device.

#### ACKNOWLEDGMENTS

The authors would like to thank the Rector of Universitas Negeri Medan for supporting this research.

#### REFERENCES

1. Gong, J., J. Liang, and K. Sumathy, *Review on dye-sensitized solar cells (DSSCs): Fundamental concepts and novel materials*. Renewable and Sustainable Energy Reviews, 2012. **16**(8): p. 5848-5860.

2. Wu, T.-L., et al., *Application of ZnO micro rods on the composite photo-electrode of dye sensitized solar cells*. *Microsystem Technologies*, 2018. **24**(1): p. 285-289.
3. Vittal, R. and K.-C. Ho, *Zinc oxide based dye-sensitized solar cells: A review*. *Renewable and Sustainable Energy Reviews*, 2017. **70**: p. 920-935.
4. Bekele, E.T., et al., *Biotemplated Synthesis of Titanium Oxide Nanoparticles in the Presence of Root Extract of Kniphofia schemperii and Its Application for Dye Sensitized Solar Cells*. *International Journal of Photoenergy*, 2021. **2021**: p. 6648325.
5. Mehmood, U., et al., *Recent Advances in Dye Sensitized Solar Cells*. *Advances in Materials Science and Engineering*, 2014. **2014**: p. 974782.
6. Roy, S., et al., *Enhanced performance of dye-sensitized solar cell with thermally stable natural dye-assisted TiO<sub>2</sub>/MnO<sub>2</sub> bilayer-assembled photoanode*. *Materials for Renewable and Sustainable Energy*, 2020. **9**.
7. Ye, M., et al., *Recent advances in dye-sensitized solar cells: from photoanodes, sensitizers and electrolytes to counter electrodes*. *Materials Today*, 2015. **18**(3): p. 155-162.
8. Sasidharan, S., et al., *Fine tuning of compact ZnO blocking layers for enhanced photovoltaic performance in ZnO based DSSCs: a detailed insight using  $\beta$  recombination, EIS, OCVD and IMVS techniques*. *New Journal of Chemistry*, 2017. **41**(3): p. 1007-1016.
9. Rashad, M., et al., *Physical and nuclear shielding properties of newly synthesized magnesium oxide and zinc oxide nanoparticles*. *Nuclear Engineering and Technology*, 2020. **52**(9): p. 2078-2084.
10. Fu, X., et al., *Large-Scale Growth of Ultrathin Low-Dimensional Perovskite Nanosheets for High-Detectivity Photodetectors*. *ACS Applied Materials & Interfaces*, 2020. **12**(2): p. 2884-2891.

11. Fang, D., et al., *Structural and optical properties of Mg-doped ZnO thin films prepared by a modified Pechini method*. Crystal Research and Technology, 2013. **48**(5): p. 265-272.
12. Lekoui, F., et al., *Elaboration and Characterization of Mg-Doped ZnO Thin Films by Thermal Evaporation: Annealing Temperature Effect*. Brazilian Journal of Physics, 2021. **51**(3): p. 544-552.
13. Jilani, A., M. Abdel-wahab, and A. Hammad, *Advance Deposition Techniques for Thin Film and Coating*. 2017.
14. Goktas, S. and A. Goktas, *A comparative study on recent progress in efficient ZnO based nanocomposite and heterojunction photocatalysts: A review*. Journal of Alloys and Compounds, 2021. **863**: p. 158734.
15. Aslan, F., et al., *Growth of ZnO nanorod arrays by one-step sol-gel process*. Journal of Sol-Gel Science and Technology, 2016. **80**(2): p. 389-395.
16. Goktas, A., A. Tumbul, and F. Aslan, *A new approach to growth of chemically depositable different ZnS nanostructures*. Journal of Sol-Gel Science and Technology, 2019. **90**(3): p. 487-497.
17. Mia, M.N.H., et al., *Influence of Mg content on tailoring optical bandgap of Mg-doped ZnO thin film prepared by sol-gel method*. Results in Physics, 2017. **7**: p. 2683-2691.
18. Arif, M., et al., *Effect of Annealing Temperature on Structural and Optical Properties of Sol-Gel-Derived ZnO Thin Films*. Journal of Electronic Materials, 2018. **47**(7): p. 3678-3684.
19. Chen, T.-H., et al., *Effects of different annealing temperature on the optoelectrical properties of MGZO thin films prepared by co-sputtering method*. Microsystem Technologies, 2019. **25**.



20. Gultom, N.S., H. Abdullah, and D.-H. Kuo, *Phase transformation of bimetal zinc nickel oxide to oxysulfide photocatalyst with its exceptional performance to evolve hydrogen*. Applied Catalysis B: Environmental, 2020. **272**: p. 118985.
21. Gultom, N.S., H. Abdullah, and D.-H. Kuo, *Facile synthesis of cobalt-doped (Zn,Ni)(O,S) as an efficient photocatalyst for hydrogen production*. Journal of the Energy Institute, 2019. **92**(5): p. 1428-1439.
22. Ertap, H. and M. Karabulut, *Structural and electrical properties of boron doped InSe single crystals*. Materials Research Express, 2018. **6**(3): p. 035901.
23. Al-Khalqi, E.M., et al., *Highly Sensitive Magnesium-Doped ZnO Nanorod pH Sensors Based on Electrolyte–Insulator–Semiconductor (EIS) Sensors*. Sensors, 2021. **21**(6).
24. Zeleke, M.A., et al., *Facile synthesis of bimetallic (In,Ga)<sub>2</sub>(O,S)<sub>3</sub> oxy-sulfide nanoflower and its enhanced photocatalytic activity for reduction of Cr(VI)*. Journal of Colloid and Interface Science, 2018. **530**: p. 567-578.
25. Goktas, A., et al., *Mg doping levels and annealing temperature induced structural, optical and electrical properties of highly c-axis oriented ZnO:Mg thin films and Al/ZnO:Mg/p-Si/Al heterojunction diode*. Thin Solid Films, 2019. **680**: p. 20-30.
26. Kurtaran, S., *Al doped ZnO thin films obtained by spray pyrolysis technique: Influence of different annealing time*. Optical Materials, 2021. **114**: p. 110908.
27. Goktas, A., et al., *Physical properties of solution processable n-type Fe and Al co-doped ZnO nanostructured thin films: Role of Al doping levels and annealing*. Materials Science in Semiconductor Processing, 2018. **75**: p. 221-233.

28. Gultom, N.S., et al., *Transforming Zn(O,S) from UV to visible-light-driven catalyst with improved hydrogen production rate: Effect of indium and heterojunction*. *Journal of Alloys and Compounds*, 2021. **869**: p. 159316.

## #Reviewer 4

This study has some interesting results. The authors have done a good job and effort to comment on the results accordingly. However, the English of the presented study is below the expectations. Further, the presented study needs to be improved according to issues given below and the reason of the obtained findings need to be commended in more details with more supportive idea and references. Moreover, it will be a good advantage to state the aim of the presented investigation. Hence, after doing the issues and suggestions accordingly as given below, this study can be recommended for possible publication in the Journal.

Thank you very much for your time and effort to review our manuscript. Now response your comments as follows,

1-There are many serious mistakes in the English grammar and writing rules (some of them are denoted in the attached file). Therefore, it is suggested to review and check the manuscript by the English grammar expertise to correct it carefully.

### **Authors reply:**

Thank you so much for your valuable suggestions. We have improved the English of our manuscript.

2- The authors have expressed that the SEM images reveal that the surface of Mg-doped ZnO thin film is nanosphere (introduction and page 5). This statement is physically not meaningful. It will be much meaningful if they state as the SEM images reveal that the grain/particle shape of the surface of the Mg-doped ZnO thin film is nanosphere. Similarly, the success of Mg-doped into ZnO host (the successful Mg doping into ZnO host)

### **Authors reply:**

Thank you for your suggestion. We have modified that sentence according to your suggestion and also the reviewer 3', as follows:

*“The SEM images reveal that particles of the surface of the Mg-doped ZnO thin film are irregular shapes.”*

3-It will be useful to enlarge the introduction according to the followings, recommended to mention them within the text, in terms of advantage and physical/chemical characterizations of the sol-gel technique and ZnO semiconductor: (i) Journal of Alloys and Compounds, 158734, 2021; (ii) Brazilian Journal of Physics volume 51, pages544–552(2021); (iii) Applied Physics A 126 (10), 2020, 1-6.

**Authors reply:**

Thank you very much for suggesting us to improve our introduction. Those references have been added in the revised manuscript.

4-Please do not start with a bigger uppercase letter (Sol-gel spin page 3) except for the after the dot. If you use any abbreviation (like XRD) please do not use the main word like x-ray diffraction. Also, please do not use the united words/items like and4

**Authors reply:**

Thank you. We have done so.

5-The authors have stated that it is also clearly seen that the intensity of X-ray diffraction increases as the temperature of annealing increased, which indicates an improvement in the crystallinity of Mg-Doped ZnO films with the rise in temperature (i) and the crystallite sizes do not clearly change for different annealing temperatures. (ii). these two statements do not agree with each other.

**Authors reply:**

Thank you for comment. Those sentences have been revised.

6- Please add or calculate peak intensity, diffraction angles, lattice parameters, micro-strain, and dislocation density of all samples. And also discuss their influences on the measured or presented properties. For the calculation and comments, it is suggested to use the followings, which will be a good advantage to mention them within the text. (i) Thin Solid Films 680, 2019, 20-30 (ii) Sensors 2021, 21(6), 2110; (iii) Materials Research Express 6 (3), 2019, 035903; (iv) Thin Solid Films, 717, 2021, 138447.

**Authors reply:**

Thank you very much for leading us to explain our XRD analysis with a deeper technique. Those relevance references have been added in the revised manuscript.

7- The followings are contradicted please correct them; (i) Therefore, the optimum temperature of annealing is 500 oC with a maximum of power conversion efficiency of 3.53%; (ii) Based on the characterization result, the highest efficiency of 3.53% at 550 oC could be contributed to its highest degree of crystallinity.

**Authors reply:**

Thank for correcting us. We have revised that statement.

8-The explanations/reasons for the variation in transmittance, absorbance, and bandgap widening by annealing temperatures need to be addressed with more details. Also, discuss about the relationship between the lattice parameters and the bandgap of the produced film samples. It is suggested to use the following for references, which will help you to explain the issue: (i) Materials Science in Semiconductor Processing 75, 221-233; (ii) Optical Mater. 114, 2021, 110908; (iii) Journal of Sol-Gel Science and Technology 90 (3), 487-497.

**Authors reply:**

Thank you very much for guiding us to explain our results with a better way. Those relevance references have been added in the revised manuscript.

At last, the authors would like to thank you reviewer for your time and valuable suggestion to improve the quality of our manuscript. We have tried our best to revise the manuscript according to your comments. Please kindly support us, by recommending the revised manuscript for publication in the journal. Thank you.

## #Reviewer 3

1. Abstract: There is a confusion by authors between crystallite/grain size vs particles size.

**Authors reply:**

Thanks for your comment. Now, it is clear for us.

2. P5: The particles have irregular shapes instead of nanospheres shapes.

**Authors reply:**

Thank you. We have modified that sentence in the revised manuscript.

3. P5: It is more appropriate to use the term “particle size” instead of “grain size” as the FESEM images would not be able to indicate that the particle only contained single grain or polygrains.

**Authors reply:**

Thank you for correcting us. We have modified in the manuscript according to your suggestion.

4. P6: It is good to have FESEM images for samples without annealing (as-deposited) and annealed at 450 oC in Figure 2 for comparison purpose.

**Authors reply:**

Thank you for your valuable suggestion. However, the authors unable to provide those data due to funding limitation and also the pandemic make difficulty to conduct experiment. Your understanding is highly appreciated.

5. P6: The present of Mg element in the EDS analysis does not mean that Mg has been successfully doped into the ZnO and they are electrically active. More evident are needed to prove that Mg has been doped into the ZnO particles.

**Authors reply:**

Thanks for your comment. The XRD did not show any peak of MgO which indicated that there was no formation of secondary phase of MgO but the peak shift about 0.75 for two theta might provide the evidence of success Mg doping into ZnO. Furthermore, we consider

with such low concentration of 1.32%, Mg as dopant more possible and reasonable to form a single phase. We also apologize that we have facility limitation to further prove Mg has been doped to ZnO.

6. P7: Please index the diffraction planes in the XRD results as shown in Figure 3.

**Authors reply:**

Thank you for great suggestion. We have indexed each peak of XRD in Figure 3.

7. P7: It is good to include the XRD of as-deposited thin film in Figure 3 for comparison purpose.

**Authors reply:**

We really appreciated your valuable suggestion. However, at present time and midst of pandemic COVID-19, it is really difficult for us to do experiment. Now, we work from home. Your understanding is highly appreciated.

8. P8: Why lower absorbance was obtained when the annealing temperature was 550 oC as shown in Figure 4?

**Authors reply:**

Thank you for your question. It is well known that there is always an optimum absorbance for different temperatures annealing. In our case, the optimum temperature was 500 to give the highest optical absorbance.

9. P9: Why the transmittances (not “transmission”) of Mg-doped ZnO thin films annealed at different temperature were random?

**Authors reply:**

Thank you for question. We have corrected that figure as in Figure 6 according to the reviewer 1’s suggestion (derived from absorption data). Now, it is reasonable.

10. P10: Why increase of particle size (not “grain size”) will caused increment in bandgap energy?

**Authors reply:**

Thank

11. P12: The highest efficiency of 3.53 % was achieved using ZnO thin film annealed at 500 oC (not 550 oC). Thus, the claim of improved degree of conductivity in this context is not correct.

**Authors reply:**

Thanks for correcting us. We have deleted that statement.

12. Suggest to highlight the problem(s) to be addressed in this paper in introduction. Also, to highlight the novelty of this work.

**Authors reply:**

Thank you for your valuable suggestion. We have modified the introduction part.

At last, the authors would like to thank you reviewer for your time and valuable suggestion to improve the quality of our manuscript. We have tried our best to revise the manuscript according to your comments. Please kindly support us, by recommending the revised manuscript for publication in the journal. Thank you.



## #Reviewer 1

This contribution reports interesting results on a ZnO-Mg based DSSC using a natural extract as photosensitizer. Yet the manuscript has serious flaws such as fill factors above 100% and the presented data does not entirely support the given conclusions. Also the english writing is very poor. I attach an annotated pdf file of the manuscript with all my comments/corrections that must be addressed before the contribution is suitable for publication. The pdf file was created using MS-Word and annotated using Okular software running under linux/KDE. I was almost rejecting this work but decided to give it a second chance.

### **Authors reply:**

Thank you very much for your time and valuable suggestion to improve the quality of our manuscript. We have tried our best to revise the manuscript according to your comments. Please kindly support us, by recommending the revised manuscript for publication. Thank you.

## Permintaan revisi ke-2 tanggal 20 Agustus 2021

Re: Your response is required: 4033692 Inbox

**Pavithra Kumar** [publication.ethics@hindawi.com](mailto:publication.ethics@hindawi.com) via [freshdesk.com](https://freshdesk.com)  
to me, motlan, gabejhp, makmur, juniastel, notosusantogultom, fedluked130

Fri, Aug 20, 1:06 PM

Dear Dr. Siregar,

I am writing to you regarding your manuscript:

Nurdin Siregar, Motlan Motlan, Jonny Haratua Panggabean, Makmur Sirait, Juniastel Rajagukguk, Noto Susanto Gultom, Fedlu Kediri Sabir, "Fabrication of dye-sensitized solar cells (DSSC) using Mg-doped ZnO as photoanode and extract of rose myrtle (*Rhodomyrtus tomentosa*) as natural dye", *International Journal of Photoenergy*, MS ID: 4033692.

Our routine internal checks identified that a reviewer has suggested the addition of citations to the handling editor and reviewers' published articles. Following our assessment, it has been determined that the citations should be removed from the manuscript in this case. I would therefore like to ask if you are willing to remove the citations, replacing them with alternatives if necessary. This is to avoid any perception of excessive citation of the Handling Editor and reviewer's published work.

The citations to be removed/replaced are:

4. Goktas, S. and A. Goktas, A comparative study on recent progress in efficient ZnO based nanocomposite and heterojunction photocatalysts: A review. *Journal of Alloys and Compounds*, 2021. 863: p. 158734.

16. Goktas, A., A. Tumbul, and F. Aslan, A new approach to growth of chemically depositable different ZnS nanostructures. *Journal of Sol-Gel Science and Technology*, 2019. 90(3): p. 487- 497.

26. Goktas, A., et al., Mg doping levels and annealing temperature induced structural, optical and electrical properties of highly c-axis oriented ZnO:Mg thin films and Al/ZnO:Mg/p-Si/Al heterojunction diode. *Thin Solid Films*, 2019. 680: p. 20-30.

28. Goktas, A., et al., Physical properties of solution processable n-type Fe and Al co-doped ZnO nanostructured thin films: Role of Al doping levels and annealing. *Materials Science in Semiconductor Processing*, 2018. 75: p. 221-233.



Submitted revisi ke-2 tanggal 24 Juni 2021



Nurdin ▾

← BACK DASHBOARD / ARTICLE DETAILS

Updated on 2021-06-24 Version 3 ▾

## Fabrication of dye-sensitized solar cells (DSSC) using Mg-doped ZnO as photoanode and extract of rose myrtle (*Rhodomyrtus tomentosa*) as natural dye

[VIEWING AN OLDER VERSION](#)

ID 4033692

Nurdin Siregar <sup>SA</sup> <sup>CA</sup> <sup>1</sup>, Mottan Motlan<sup>1</sup>, Jonny Haratua Panggabean<sup>1</sup>, Makmur Sirait<sup>1</sup>, Juniastel Rajaguguk<sup>1</sup>, Noto Susanto Gultom<sup>1</sup>, Fedlu Kedir Sabir<sup>2</sup> + [Show Affiliations](#)

### Article Type

Research Article

### Journal

International Journal of Photoenergy

Chief Editor Giulia Grancini

Academic Editor Carneiro Joaquim

Submitted on 2021-06-24 (3 months ago)

> Abstract

> Author Declaration

▼ Files 3

#### Main manuscript

Manuscript\_clean\_2nd.docx

4 MB



#### Cover letter

Cover letter\_2nd revised.docx

14 kB



#### Supplemental files

Manuscript\_mark up\_2nd revision.docx

4 MB



## **Fabrication of dye-sensitized solar cells (DSSC) using Mg-doped ZnO as photoanode and extract of rose myrtle (*Rhodomyrtus tomentosa*) as natural dye**

Nurdin Siregar<sup>1\*</sup>, Motlan<sup>1</sup>, Jonny Haratua Panggabean<sup>1</sup>, Makmur Sirait<sup>1</sup>, Juniastel Rajagukguk<sup>1</sup>, Noto Susanto Gultom<sup>1</sup>, Fedlu Kediri Sabir<sup>2</sup>.

<sup>1</sup>Department of Physics, Faculty of Mathematics and Natural Sciences, State University of Medan, Jl. Willem Iskandar Pasar Medan Estate, Medan 20221, Indonesia

<sup>2</sup>Department of Applied Chemistry, School of Applied Natural Science, Adama Science and Technology University, P.O. Box 1888, Adama, Ethiopia

\*Corresponding author: [siregarnurdin@unimed.ac.id](mailto:siregarnurdin@unimed.ac.id)

### **ABSTRACT**

A dye-sensitized solar cell (DSSC) device using Mg-doped Zn thin films as photoanode and fruit extract of rose myrtle (*Rhodomyrtus tomentosa*) as the natural dye was investigated. The effect of annealing temperature (400-550 °C) on the films of photoanode was systematically studied using an X-ray diffractometer (XRD), UV-Visible Near Infrared (UV-Vis NIR) Spectrophotometer, scanning electron microscopy (SEM), and energy dispersive spectroscopy (EDS). XRD confirm that all sample has the wurtzite hexagonal with crystallite size of 25 nm. The SEM images reveal that particles ~~on~~ of the surface of the Mg-doped ZnO thin film ~~of~~ are irregular shapes. Increasing the annealing temperature leads to a larger particle size and slightly increases bandgap energy. The dye sensitizer of extracted rose myrtle (*Rhodomyrtus tomentosa*) has a strong absorption at the visible light region. The maximum efficiency of the DSSC device is 3.53% with Mg-ZnO photoanode annealed at 500 °C.

**Keywords:** Dye Sensitized Solar Cell, Mg-doped ZnO, sol-gel spin coating, natural dye

## 1. INTRODUCTION

The demands for renewable energy continually increase every year due to its eco-friendliness. Solar cells have been well known as a device to convert solar energy to electricity for decades. However, the conventional solar cells are still high price due to complicated fabrication process and expensive of raw materials. Dye-sensitized solar cell (DSSC), is one of the most promising solar cell types to produce renewable energy with a low-cost material and simple fabrication process [1-3]. After irradiation, the dye sensitizer harvests light and causes an electron to promote the conduction band leaving a hole in the valence band. There are numerous pigments of plant leaves, fruits, and flowers that have the potential to be utilized in DSSC. The variety of pigments with different absorption wavelengths and degrees of absorptivity in UV-Visible spectrum can cause different performances of DSSC. The molecules of the dye can be anchored into the surface areas of the semiconductor to form Lewis acid-base types of interaction to enhance electron transfer from HOMO of the dye molecule (pigment) to the conduction band of the semiconductor (anode) [4-7].

Zinc oxide (ZnO) semiconductor plays an important role as a photoanode to improve the conducting interface layer and to enhance the power conversion efficiency (PCE). According to the literature, ZnO has a high electron mobility, wide bandgap (3.37eV), and large exciton binding energy of 60 meV [8]. Magnesium (Mg) is one of the metals that is used in many applications such as refractory materials, optical and heating apparatus [9, 10]. Mg-doped ZnO material also has special properties to block the electron due to of its wide bandgap [11, 12]. There are several methods to grow thin film on a substrate, such as molecular beam epitaxy, metal organic chemical vapor deposition, plasma enhanced chemical deposition, sputtering method, spray pyrolysis, atomic layer deposition, pulse laser deposition, electron beam evaporation, and sol-gel [13]. The sol-gel method has several advantages compared to aforementioned methods such as simple, cheap, and efficient [14-16]. By using a sol-gel spin coating

technique, several parameters like concentration of precursor solution, annealing temperature, annealing time, and so on can be easily tuned in order to achieve the desired properties[12, 17].

In this work, the photoanodes of Mg-doped ZnO thin films were prepared by a sol-gel spin coating method. To the best of our knowledge, the natural dye from the fruit extract of *Rhodomyrtus tomentosa* has not been reported yet as the dye sensitizer for DSSC. The effect of different annealing temperatures on structural and optical properties of Mg-doped ZnO photoanodes as well as the efficiency of DSSC device was systematically investigated using necessary characterization tools. We find that the maximum efficiency of the DSSC device is 3.53% with Mg-doped ZnO photoanode annealed at 500 °C.

## **2. EXPERIMENTAL SECTION**

### **2.1. Synthesis of Mg-doped ZnO thin films**

Mg-doped ZnO thin films were fabricated using a sol-gel spin coating technique. Typically, zinc Acetate dehydrate and magnesium chloride (2 wt.%) were dissolved in isopropanol (35 mL) under continuous stirring. After 10 min, 1.7 mL diethanolamine was added slowly into the solution. After refluxing process at 90 °C for about 2 hours, the gel was dropped on top of FTO glass and spun at 5000 rpm for 60 s. After the drying process, the samples were annealed at different temperatures of 400, 450, 500, and 550°C for 5 hours.

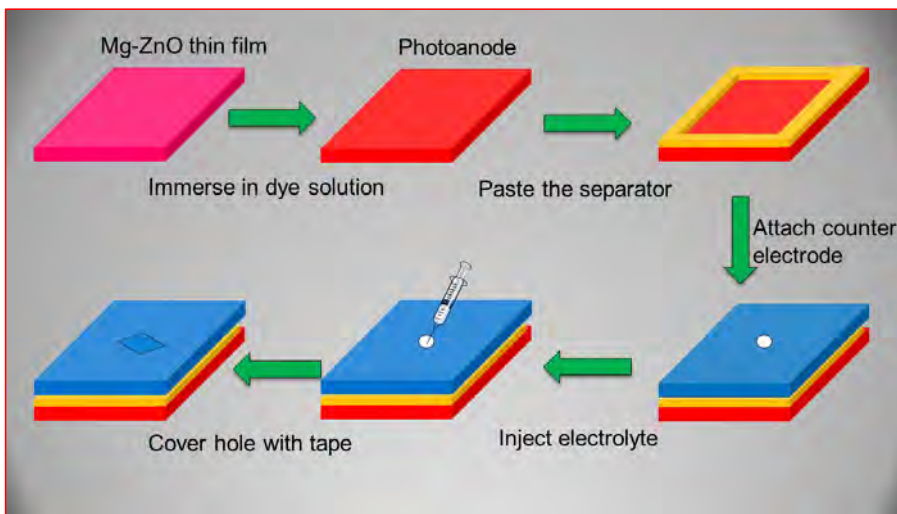
### **2.2. Extraction of natural dyes**

About 50 grams of *Rhodomyrtus tomentosa* fruit was ground using a mortar. After being moved into a beaker glass, 25 mL DI water, 21 mL ethanol, and 4 mL acetic acid were added and then stirred to form a homogeneous solution. The solution was then covered with aluminum foil to avoid photooxidation and soaked at room temperature for 24 h. Finally, the solid and liquid parts were separated using filter paper.

The filtered solution of *Rhodomyrtus tomentosa* fruit extract was ready to be used as the sensitizer in DSSCs.

### 2.3. Fabrication of DSSC

Figure 1 illustrates the schematic fabrication of the DSSC device. First, the as-prepared Mg-doped ZnO thin film was used as the photoanode electrode. Natural-dye sensitized from *Rhodomyrtus tomentosa* fruit extract was adsorbed on the top of Mg-doped ZnO photoanode by immersing it into the extracted dye solution for several hours. After that, it was taken out and washed with ethanol to remove the unadsorbed dye and dried in the oven at 80 °C. The commercial platinum coated on the glass FTO was used as the counter electrode. The DSSCs were assembled by attaching the photoanode and the counter electrode using thermoplastic sealant surlyn as glue and separator. And then heated at 80 °C to let the surlyn perfectly attach to the electrodes. The electrolyte was injected through a tiny hole on that was drilled on the counter electrode. Finally, that hole was covered with transparent tape.





**Figure 1.** Schematic of the fabrication of DSSC using Mg-doped ZnO photoanode and fruit extract of *Rhodomyrtus tomentosa*.

#### 2.4. Characterization tools

To observe the surface morphology of Mg-doped ZnO thin films annealed at different temperatures, a scanning electron microscope (JEOL-6500) analysis was performed at an accelerating voltage of 15 kV. The X-ray diffraction (XRD) pattern of Mg-doped ZnO thin films were analyzed using an X-ray diffractometer (LabX XRD-6100, Shimadzu) with Cu K $\alpha$  ( $\lambda=1.54$  Å). The transmittance and absorbance spectra were recorded using a UV-Vis NIR spectrophotometer. The efficiency of the DSSC was measured using an I-V measurement (Keithly Source Measure Unit) system by irradiating a photoanode electrode with a LED and input power of 35 mW/cm<sup>2</sup>. Several data such as open-circuit voltage ( $V_{oc}$ ), short circuit current density ( $J_{sc}$ ), maximum voltage ( $V_{max}$ ), and maximum current ( $J_{max}$ ) were recorded. Then, the fill factor (FF) and efficiency ( $\eta$ ) were determined using equations (1) and (2), respectively.

$$FF = \frac{J_{max} \times V_{max}}{J_{sc} \times V_{oc}} \quad (1)$$

$$\eta = FF \frac{J_{sc} \times V_{oc}}{P_{in}} \times 100\% \quad (2)$$

### 3. RESULTS AND DISCUSSION

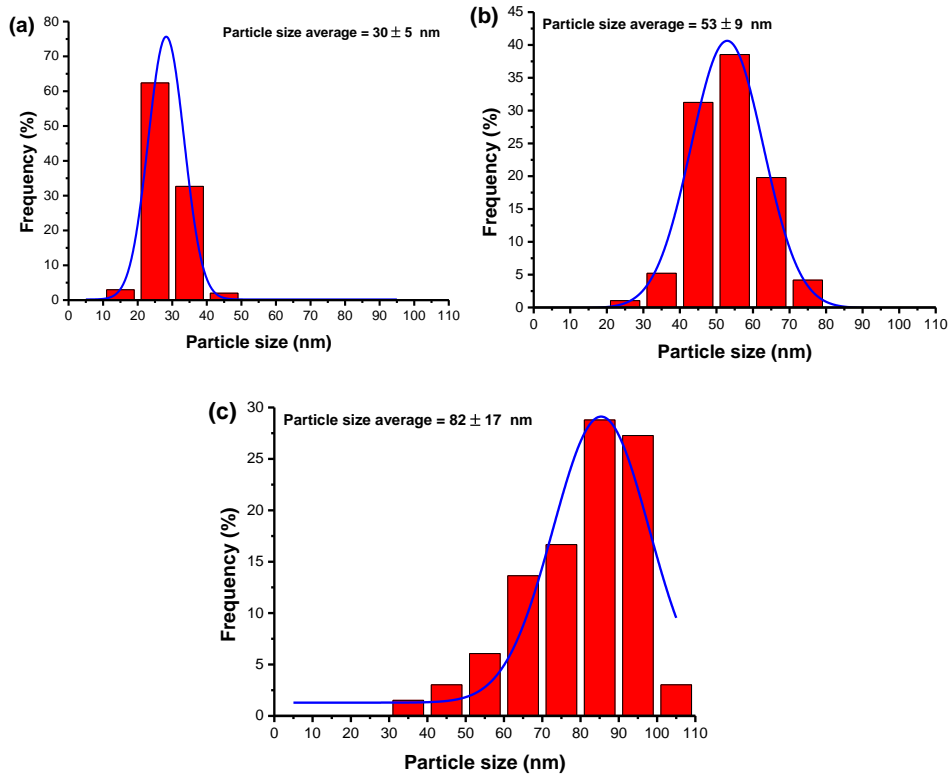
#### 3.1. Electron microscope analysis

The surface morphology of Mg-doped ZnO with variation of annealing temperatures was investigated using a field-emission scanning electron microscope. With a magnification of 30 k times, the top view images of Mg-doped ZnO thin films can be clearly observed in Figure 2. The surface microstructure of Mg-doped ZnO at different annealing temperatures shows nanoparticles with irregular shapes. It was clearly observed that by increasing the annealing temperature, the particle size was monotonically



**Figure 2.** Scanning electron microscope images of Mg-doped ZnO with variation of annealing temperatures. (a) 400, (b) 500, (c) 550, and (d) representative EDS analysis

To calculate the particle size more precisely, further analysis was conducted using image-J analysis. As shown in Figure 3a-c, the average particle sizes for Mg-doped ZnO thin films annealed at 400, 500, and 550 °C are  $30 \pm 5$ ,  $53 \pm 9$ , and  $82 \pm 17$  nm, respectively. A larger particle size at a higher annealing temperature was reasonable. It could be explained due to a higher driving force from thermal energy that leads to a faster particle growth through Ostwald ripening mechanism. Our findings also well agree with some previous reports [18, 19].

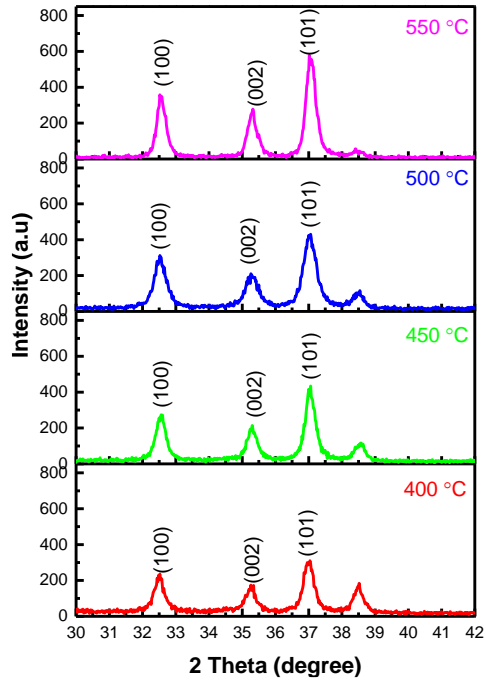


**Figure 3.** Particle size distribution of Mg-doped ZnO annealed at (a) 400, (b) 500, and (c) 550 °C

### 3.2. XRD analyses

The crystal properties of Mg-doped ZnO were studied by XRD technique. The results are shown in Figure 4. The XRD patterns are similar to a wurtzite crystal structure based on the standard card of JCPDF #36-1451 (ZnO) [20]. Three peaks that located at  $32.5^\circ$ ,  $35.3^\circ$ , and  $37.0^\circ$  for  $2\theta$  could be assigned as (100), (001) and (101) planes of ZnO, respectively. The other weak peak at about  $38.5^\circ$  might be contributed by impurity as reported in the previous work [21]. The intensity of peaks in Figure 4 gradually elevates as

the temperature of annealing increase, which indicates an improvement in the crystallinity of Mg-Doped ZnO films.



**Figure 4.** XRD pattern of Mg-doped ZnO thin films at different annealing temperatures.

Table 1 lists the summary of structural properties of Mg-doped ZnO thin films at different annealing temperatures. The average crystallite size of Mg-doped ZnO thin films was calculated at (101) plane using Scherer formula as shown in equation (3) [22]. Their crystallite size values are 20.60, 21.23, 16.83, and 22.9 nm at the annealing temperature of 400, 450, 500, and 550 °C, respectively. Next, the dislocation density ( $\delta$ ) of Mg-doped ZnO was further determined by equation (4) [23]. The dislocation density of Mg-doped ZnO annealed at 400, 450, 500 and 550 °C are  $2.36 \times 10^{-3}$ ,  $2.22 \times 10^{-3}$ ,  $3.53 \times 10^{-3}$ , and  $1.89 \times 10^{-3} \text{ nm}^{-2}$ , respectively. Mg-doped ZnO annealed at 500 °C has the highest dislocation density compared

to other samples. Macrostrain value that indicates the peak shift position was calculated according to equation (5) [24]. Based on the database, the (101) plane for ZnO located at 36.25 ° with an interplanar spacing of 2.4759 Å. However, the (101) plane for our Mg-doped ZnO is found at about 37.00 ° for 2θ with a calculated interplanar spacing of 2.4272 Å. The peak shifting of about 0.75 ° for 2θ also indicates that Mg as a dopant has been successfully doped into ZnO host lattice [25]. The macrostrain value was similar for different temperatures with a value of 1.97 x 10<sup>-2</sup> because of their similarity in peak position. Based on the previous reports [26, 27], the lattice parameters *a* and *c* of Mg-doped ZnO were estimated to be about 3.172 Å and 5.080 Å using equations (6) and (7), respectively. The lattice parameter *a* at (100) plane did not significantly different for different annealing temperatures because their peak position was located almost in the same diffraction angle. Similarly, the lattice parameter *c* at (002) plane also very similar at different annealing temperatures, as listed in Table 1.

$$D = \frac{0.9\lambda}{\beta \cos \theta} \quad (3)$$

Where, D is the crystallite size (nm), λ is the wavelength (nm), β is the full half maximum, FWHM (rad), and θ is Bragg angle (°).

$$\delta = \frac{1}{D^2} \quad (4)$$

$$\langle e \rangle = \frac{d-d_0}{d_0} \quad (5)$$

Where, d<sub>0</sub> is the interplanar spacing of pure ZnO without deformation while d is the calculated interplanar spacing for Mg-doped ZnO at (101) plane using Bragg law.

$$a = \frac{\lambda}{\sqrt{3} \sin \theta_{(100)}} \quad (6)$$

$$c = \frac{\lambda}{\sin \theta_{(002)}} \quad (7)$$

**Table 1.** Summary of crystal properties of FWHM, crystallite size, dislocation density, macrostrain values, and lattice parameters (*a* and *c*) of Mg-doped ZnO thin films at different annealing temperatures.

Temperature (°C)	FWHM/ $\beta$ (rad)	Crystallite size (nm)	Dislocation density $\times 10^{-3}$ (nm <sup>-2</sup> )	Macro strain values $\langle e \rangle$	Lattice parameters (Å)	
					<i>a</i>	<i>c</i>
400	0.4065	20.60	2.36	$1.97 \times 10^{-2}$	3.176	5.082
450	0.3945	21.23	2.22	$1.97 \times 10^{-2}$	3.172	5.080
500	0.4976	16.83	3.53	$1.97 \times 10^{-2}$	3.175	5.083
550	0.3645	22.9	1.89	$1.97 \times 10^{-2}$	3.173	5.080

### 3.2. Optical properties

To study the effect of different annealing temperatures on optical properties, the absorption and transmission spectra of Mg-doped ZnO thin films were measured and presented in Figure 5 and Figure 6, respectively. The absorption peaks of all Mg-doped ZnO thin films are located at a wavelength of 350 nm, which is at the UV region. As clearly shown in Figure 5, the absorption of Mg-doped ZnO annealed at 400 °C is quite low. However, after increasing the annealing temperature to 450 °C and 500 °C the absorption sharply elevates. Further increasing the temperature of annealing to 550 °C leads to a lower absorbance but still higher than that at 400 °C. Figure 6 exhibits transmission spectra of Mg-doped ZnO which also shows a similar trend to the absorption spectra in Figure 5. The thin films have transparency about 50-80 % at visible light region.

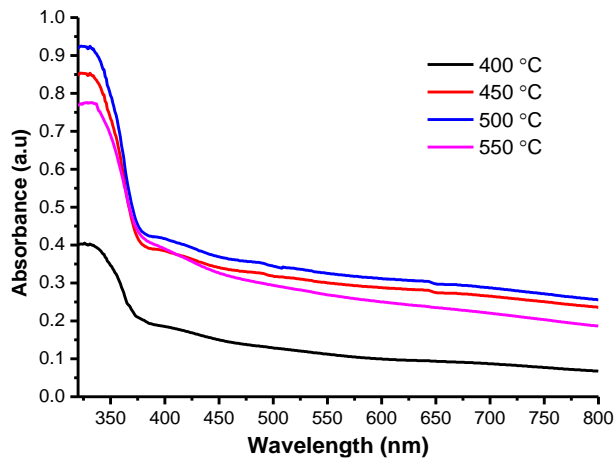


Figure 5. Absorbance spectra of Mg-doped ZnO thin films at different annealing temperatures.

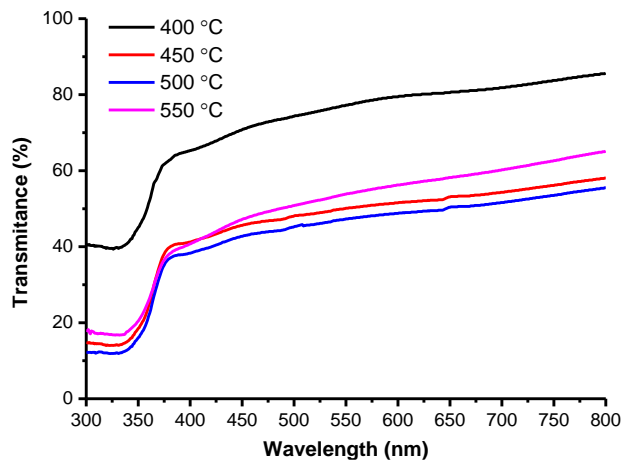
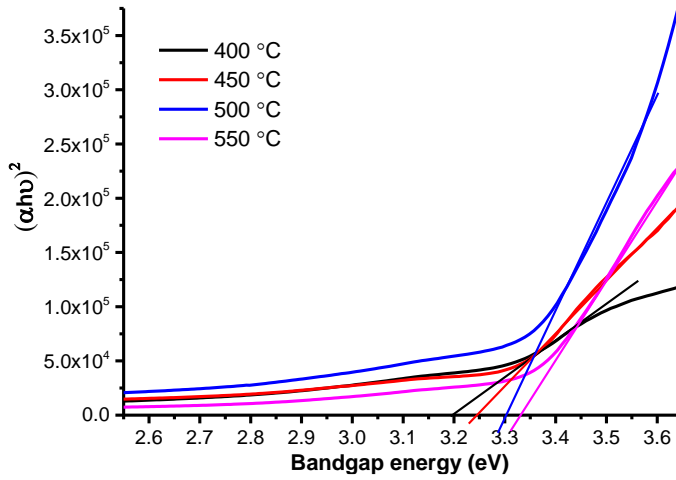


Figure 6. Transmittance spectrum of Mg-doped ZnO thin films at different annealing temperatures.



The bandgap energy of Mg-doped ZnO thin films was further derived based on the optical absorption data and plotted in Figure 7. As listed in Table in 2, bandgap energy values are 3.20, 3.24, 3.30, and 3.33 eV for annealing at 400, 450, 500, and 550, °C respectively. The slight increment of bandgap energy with increasing temperature might be due to the Burstein–Moss effect as reported in previous studies [26, 28].



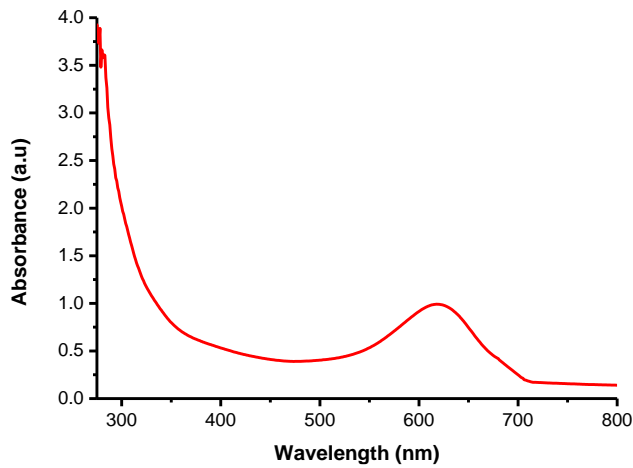
**Figure 7.** Tauc plot of Mg-doped ZnO thin films at different annealing temperatures.

**Table 2.** Bandgap energy of Mg-doped ZnO thin film at different annealing temperatures.

Temperature (°C)	Bandgap energy (eV)
400	3.20
450	3.24
500	3.30
550	3.33

### 3.4. Absorbance of *Rhodomyrtus tomentosa* dye extract

The optical absorption spectrum of the extracted rose myrtle (*Rhodomyrtus tomentosa*) natural dye was measured using a UV-Vis spectrophotometer to investigate its sensitivity to light. As shown in Figure 8, the natural dye has a strong absorption at the visible-light region with an intense absorbance peak at a wavelength of 610 nm. This property is very useful for DSSC to improve the light absorption ability. It is also well known that about 43% of the solar spectrum falls in the visible light range and only 4% is in the UV region [29]. The more light can be absorbed, the more electron-hole can be generated, which leads to a higher efficiency of a DSSC device.

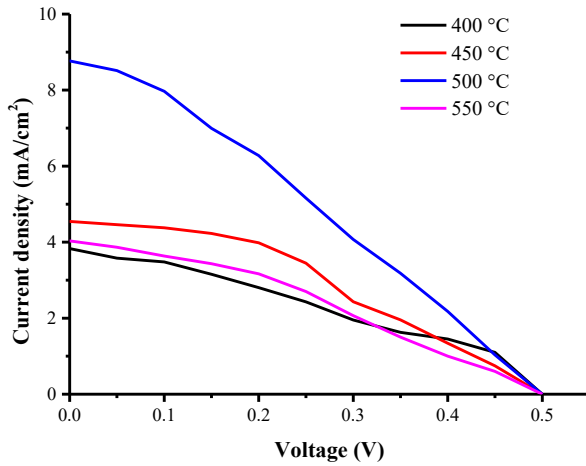


**Figure 8.** Absorbance spectrum of natural dye of extracted rose myrtle (*Rhodomyrtus tomentosa*).

### 3.5. Efficiency of DSSC

Figure 9 exhibits the  $J$ - $V$  characteristic curve of DSSC with Mg-doped ZnO as photoanode at different annealing temperatures and the fruit extract of *Rhodomyrtus tomentosa* as a natural dye sensitizer. Further, the photovoltaic properties of DSSC are listed in Table 3. The open-circuit voltage ( $V_{oc}$ ) at different annealing temperatures was similar with a value of 0.5 V. In contrast, the short-circuit current ( $J_{sc}$ ) was significantly different. The  $J_{sc}$  values are 3.83, 4.55, 8.77, and 4.03 mA/cm<sup>2</sup> at annealing temperatures of

400, 450, 500, and 550 °C, respectively. The efficiency of the DSSC device annealed at 400 °C was about 1.66%. By increasing the annealing temperature to 450 °C the efficiency also was increased to 2.36 %. Further increasing the annealing temperature to 500 °C, the efficiency of 3.53 % can be achieved. However, the efficiency was observed to decline when the annealing temperature is 550 °C. Therefore, the optimum annealing temperature is 500 °C with a maximum power conversion efficiency of 3.53%. Based on the characterization results, the highest efficiency of 3.53% at 500 °C could be contributed due to its highest optical absorption as revealed by UV-Vis analysis in Figure 5.



**Figure 9.** *J-V* characteristic curve of DSSC using Mg-doped ZnO as photoanode at different annealing temperatures.

**Table 3.** Summary of electrical properties including open-circuit voltage, short-circuit current, fill factor, and efficiency of DSSC for different annealing temperatures.

Temperature (°C)	$V_{oc}$ (V)	$J_{sc}$ (mA/cm <sup>2</sup> )	$P_{max}$ (mW/cm <sup>2</sup> )	FF (%)	$\eta$ (%)
400	0.5	3.83	0.61	31.70	1.66
450	0.5	4.55	0.86	37.93	2.36

500	0.5	8.77	1.29	29.42	3.53
550	0.5	4.03	0.68	33.47	1.85

#### 4. CONCLUSIONS

We have successfully fabricated a dye-sensitized solar cell (DSSC) device using Mg-doped ZnO thin film as the photoanode and natural dye of rose myrtle (*Rhodomyrtus tomentosa*) as the dye sensitizer. The scanning electron microscope analysis revealed that the surface of Mg-doped ZnO thin film was particles with irregular shapes. It is found that increasing the annealing temperature led to a larger particle size and slightly increased bandgap energy. The natural rose myrtle dye sensitizer had a strong absorption at the visible light region. The maximum efficiency of the DSSC device was 3.53% at an annealing temperature of 500 °C. This work demonstrates that the annealing temperature of photoanode significantly affects the efficiency of the DSSC device.

#### ACKNOWLEDGMENTS

The authors would like to thank the Rector of Universitas Negeri Medan for supporting this research.

#### REFERENCES

1. Gong, J., J. Liang, and K. Sumathy, *Review on dye-sensitized solar cells (DSSCs): Fundamental concepts and novel materials*. Renewable and Sustainable Energy Reviews, 2012. **16**(8): p. 5848-5860.
2. Wu, T.-L., et al., *Application of ZnO micro rods on the composite photo-electrode of dye sensitized solar cells*. Microsystem Technologies, 2018. **24**(1): p. 285-289.
3. Vittal, R. and K.-C. Ho, *Zinc oxide based dye-sensitized solar cells: A review*. Renewable and Sustainable Energy Reviews, 2017. **70**: p. 920-935.

4. Bekele, E.T., et al., *Biotemplated Synthesis of Titanium Oxide Nanoparticles in the Presence of Root Extract of *Kniphofia schemperii* and Its Application for Dye Sensitized Solar Cells*. International Journal of Photoenergy, 2021. **2021**: p. 6648325.
5. Mehmood, U., et al., *Recent Advances in Dye Sensitized Solar Cells*. Advances in Materials Science and Engineering, 2014. **2014**: p. 974782.
6. Roy, S., et al., *Enhanced performance of dye-sensitized solar cell with thermally stable natural dye-assisted TiO<sub>2</sub>/MnO<sub>2</sub> bilayer-assembled photoanode*. Materials for Renewable and Sustainable Energy, 2020. **9**.
7. Ye, M., et al., *Recent advances in dye-sensitized solar cells: from photoanodes, sensitizers and electrolytes to counter electrodes*. Materials Today, 2015. **18**(3): p. 155-162.
8. Sasidharan, S., et al., *Fine tuning of compact ZnO blocking layers for enhanced photovoltaic performance in ZnO based DSSCs: a detailed insight using  $\beta$  recombination, EIS, OCVD and IMVS techniques*. New Journal of Chemistry, 2017. **41**(3): p. 1007-1016.
9. Rashad, M., et al., *Physical and nuclear shielding properties of newly synthesized magnesium oxide and zinc oxide nanoparticles*. Nuclear Engineering and Technology, 2020. **52**(9): p. 2078-2084.
10. Fu, X., et al., *Large-Scale Growth of Ultrathin Low-Dimensional Perovskite Nanosheets for High-Detectivity Photodetectors*. ACS Applied Materials & Interfaces, 2020. **12**(2): p. 2884-2891.
11. Fang, D., et al., *Structural and optical properties of Mg-doped ZnO thin films prepared by a modified Pechini method*. Crystal Research and Technology, 2013. **48**(5): p. 265-272.
12. Lekoui, F., et al., *Elaboration and Characterization of Mg-Doped ZnO Thin Films by Thermal Evaporation: Annealing Temperature Effect*. Brazilian Journal of Physics, 2021. **51**(3): p. 544-552.

13. Jilani, A., M. Abdel-wahab, and A. Hammad, *Advance Deposition Techniques for Thin Film and Coating*. 2017.
14. Goktas, S. and A. Goktas, *A comparative study on recent progress in efficient ZnO based nanocomposite and heterojunction photocatalysts: A review*. Journal of Alloys and Compounds, 2021. **863**: p. 158734.
15. Aslan, F., et al., *Growth of ZnO nanorod arrays by one-step sol-gel process*. Journal of Sol-Gel Science and Technology, 2016. **80**(2): p. 389-395.
16. Goktas, A., A. Tumbul, and F. Aslan, *A new approach to growth of chemically depositable different ZnS nanostructures*. Journal of Sol-Gel Science and Technology, 2019. **90**(3): p. 487-497.
17. Mia, M.N.H., et al., *Influence of Mg content on tailoring optical bandgap of Mg-doped ZnO thin film prepared by sol-gel method*. Results in Physics, 2017. **7**: p. 2683-2691.
18. Arif, M., et al., *Effect of Annealing Temperature on Structural and Optical Properties of Sol-Gel-Derived ZnO Thin Films*. Journal of Electronic Materials, 2018. **47**(7): p. 3678-3684.
19. Chen, T.-H., et al., *Effects of different annealing temperature on the optoelectrical properties of MGZO thin films prepared by co-sputtering method*. Microsystem Technologies, 2019. **25**.
20. Gultom, N.S., H. Abdullah, and D.-H. Kuo, *Phase transformation of bimetal zinc nickel oxide to oxysulfide photocatalyst with its exceptional performance to evolve hydrogen*. Applied Catalysis B: Environmental, 2020. **272**: p. 118985.
21. Konne, J.L. and B.O. Christopher, *Sol-Gel Syntheses of Zinc Oxide and Hydrogenated Zinc Oxide (ZnO:H) Phases*. Journal of Nanotechnology, 2017. **2017**: p. 5219850.

22. Gultom, N.S., H. Abdullah, and D.-H. Kuo, *Facile synthesis of cobalt-doped (Zn,Ni)(O,S) as an efficient photocatalyst for hydrogen production*. Journal of the Energy Institute, 2019. **92**(5): p. 1428-1439.
23. Ertap, H. and M. Karabulut, *Structural and electrical properties of boron doped InSe single crystals*. Materials Research Express, 2018. **6**(3): p. 035901.
24. Al-Khalqi, E.M., et al., *Highly Sensitive Magnesium-Doped ZnO Nanorod pH Sensors Based on Electrolyte–Insulator–Semiconductor (EIS) Sensors*. Sensors, 2021. **21**(6).
25. Zeleke, M.A., et al., *Facile synthesis of bimetallic (In,Ga)<sub>2</sub>(O,S)<sub>3</sub> oxy-sulfide nanoflower and its enhanced photocatalytic activity for reduction of Cr(VI)*. Journal of Colloid and Interface Science, 2018. **530**: p. 567-578.
26. Goktas, A., et al., *Mg doping levels and annealing temperature induced structural, optical and electrical properties of highly c-axis oriented ZnO:Mg thin films and Al/ZnO:Mg/p-Si/Al heterojunction diode*. Thin Solid Films, 2019. **680**: p. 20-30.
27. Kurtaran, S., *Al doped ZnO thin films obtained by spray pyrolysis technique: Influence of different annealing time*. Optical Materials, 2021. **114**: p. 110908.
28. Goktas, A., et al., *Physical properties of solution processable n-type Fe and Al co-doped ZnO nanostructured thin films: Role of Al doping levels and annealing*. Materials Science in Semiconductor Processing, 2018. **75**: p. 221-233.
29. Gultom, N.S., et al., *Transforming Zn(O,S) from UV to visible-light-driven catalyst with improved hydrogen production rate: Effect of indium and heterojunction*. Journal of Alloys and Compounds, 2021. **869**: p. 159316.

#### #Reviewer 4

The authors did well and detailed revisions according to the eminent reviewer suggestions. Their revisions are enough and appreciable for accepting it as a possible paper in Journal. Therefore, I recommended the acceptance of the revised manuscript in International Journal of Photoenergy.

#### Authors reply:

Thank you so much for your appreciation. Your recommendation for publication is highly appreciated.

#### #Reviewer 3

The authors are not answered the following questions satisfactory.

#### Authors reply:

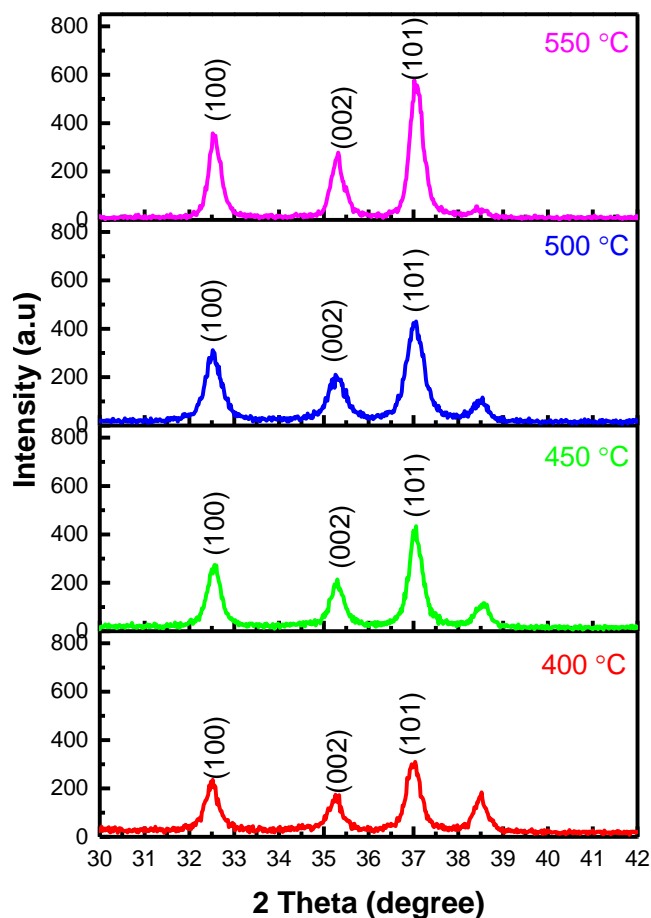
The authors do apologize for not properly answer your questions. Thank you very much again for your time and valuable suggestion in reviewing our manuscript.

Q6: P7: The diffraction planes in the XRD results are NOT indexed correctly (Figure 3).

#### Authors reply:

We are sorry for this issue. After carefully analyzed the data, we have re-indexed each peak of XRD in Figure 4.

Three peaks that located at 32.5°, 35.3°, and 37.0° for 2θ could be assigned as (100), (002) and (101) planes, respectively. The other peak at about 38.5° might be contributed by impurity as reported in the previous work [21].





Q8: P8: The reply from authors on “Why lower absorbance was obtained when the annealing temperature was 550 oC as shown in Figure 4?” is not satisfactory.

**Authors reply:**

We do sorry for not answering properly. After analyzing all our characterization results, the main difference between sample annealed at 550°C with other temperatures is the surface morphology, where Mg-ZnO thin film annealed at 550 °C had much more irregular shapes as compared to that 400 and 500 °C. So, we speculate that surface morphology is the main reason for its lower absorbance. Please help and let us know if you have other opinion. Thank you.

Q10: P10: No reply on “Why increase of particle size (not “grain size”) will caused increment in bandgap energy?”

**Authors reply:**

We do apologize for not answering this question properly. We have revised that sentence in the revise manuscript according to reviewer 1’ suggestion. As follows:

*“The bandgap energy of Mg-doped ZnO thin films was further derived based on the optical absorption data and plotted in Figure 7. As listed in Table in 2, bandgap energy values are 3.20, 3.24, 3.30, and 3.33 eV for annealing at 400, 450, 500, and 550, °C respectively. The slight increment of bandgap energy with increasing temperature might be due to the Burstein–Moss effect as reported in previous studies [1, 2].”*

Please kindly support us by recommending this second revised manuscript for publication. Thank you so much for your attention.

**#Reviewer 1**

The authors have complied to most of my suggestions / comments. Only minor issues remain that I include in an annotated pdf file. After these small corrections this manuscript is suitable for publication.

**Authors reply:**

Thank you very much again for your time and valuable suggestion to improve the quality of our manuscript. We have revised the manuscript according to your minor comments. Your recommendation for publication is highly appreciated.

#1. The platinum coated on the glass FTO Is this commercial?

Authors reply: Yes, it was commercial.

#2. This figure is not reference in the text. How were particle size selected? Was it manually? Some of the particles used to construct the histogram should be marked in the SEM figures.


Authors reply: Yes, it was manually. We have done so.

Di accepted untuk publikasi tanggal 21 Agustus 2021

4033692: Article Processing Charges Inbox x

Hindawi Invoicing <invoices@hindawi.com>  
to me ▾

Sat, Aug 21, 6:35 PM ☆ ↶ ⋮

  
Hindawi

Dear Dr. Nurdin Siregar,

**Thank you for choosing Hindawi to publish your manuscript**

We are pleased to inform you that your manuscript, Fabrication of dye-sensitized solar cells (DSSC) using Mg-doped ZnO as photoanode and extract of rose myrtle (*Rhodomyrtus tomentosa*) as natural dye, **has been accepted for publication in the journal, International Journal of Photoenergy.** We will be in touch shortly to request electronic files for your manuscript.

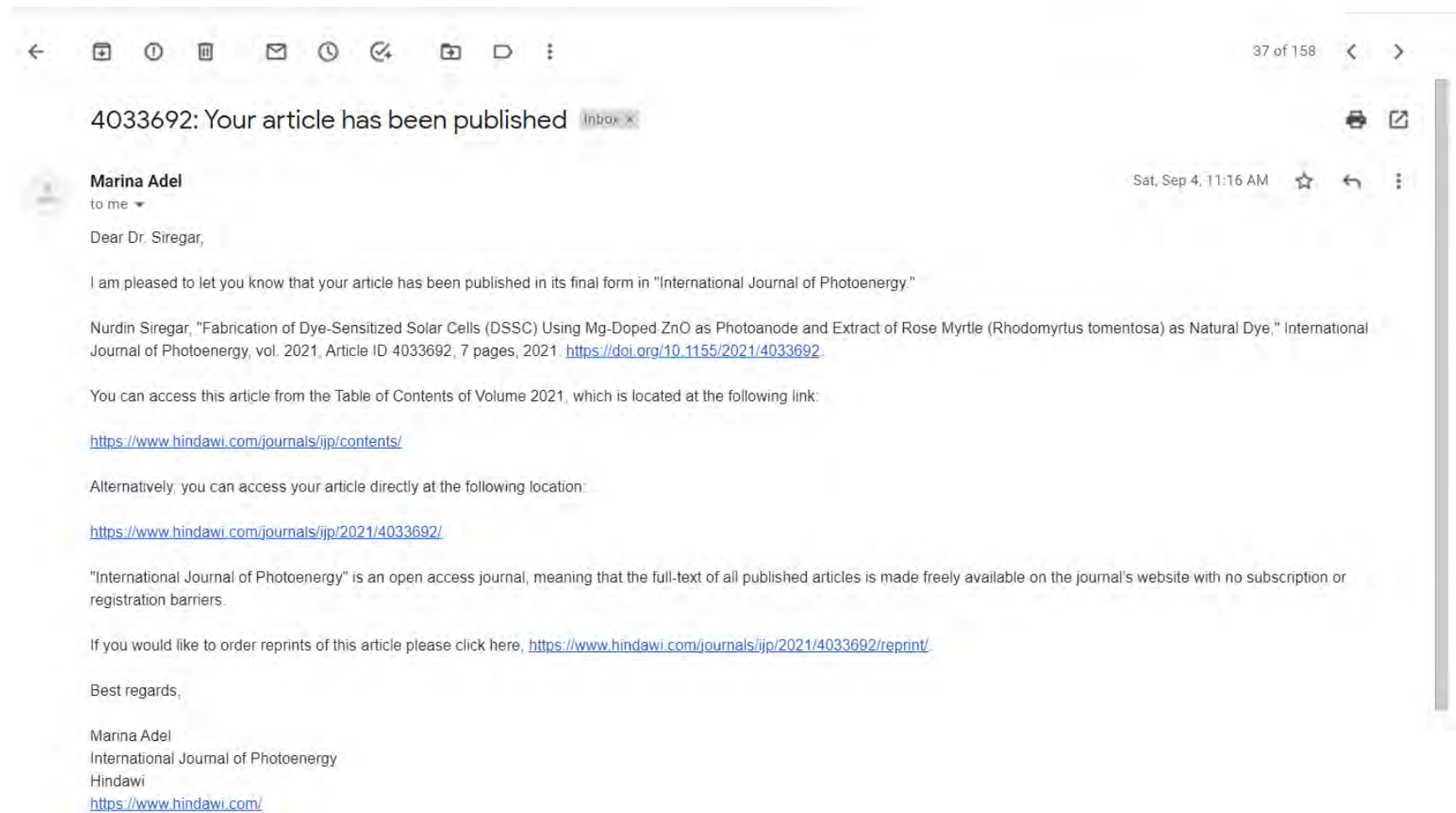
The publication process will begin upon the receipt of these files.

As an open access journal, International Journal of Photoenergy has an associated Article Processing Charge. The total charges for your manuscript 4033692, before any taxes, are USD 1800.

VAT charges will be applied for individuals resident in the UK and for institutions registered in the UK. VAT is calculated at the applicable rate, currently 20%, on the net USD amount and this VAT charge will be available for review on the invoice prior to


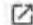






**Published tanggal 4 september 2021**



The image shows a screenshot of an email client interface. At the top, there is a navigation bar with icons for back, forward, search, and other functions. The main content area displays an email from Marina Adel. The subject line is "4033692: Your article has been published". The email body contains a message from Marina Adel to Dr. Siregar, informing him that his article has been published in the International Journal of Photoenergy. The article title is "Fabrication of Dye-Sensitized Solar Cells (DSSC) Using Mg-Doped ZnO as Photoanode and Extract of Rose Myrtle (Rhodomyrtus tomentosa) as Natural Dye." The email also provides links to access the article and order reprints.

37 of 158 < >

4033692: Your article has been published Inbox X  

 **Marina Adel**  
to me ▾ Sat, Sep 4, 11:16 AM   

Dear Dr. Siregar,

I am pleased to let you know that your article has been published in its final form in "International Journal of Photoenergy."

Nurdin Siregar, "Fabrication of Dye-Sensitized Solar Cells (DSSC) Using Mg-Doped ZnO as Photoanode and Extract of Rose Myrtle (Rhodomyrtus tomentosa) as Natural Dye," International Journal of Photoenergy, vol. 2021, Article ID 4033692, 7 pages, 2021. <https://doi.org/10.1155/2021/4033692>.

You can access this article from the Table of Contents of Volume 2021, which is located at the following link:

<https://www.hindawi.com/journals/ijp/contents/>

Alternatively, you can access your article directly at the following location:

<https://www.hindawi.com/journals/ijp/2021/4033692/>

"International Journal of Photoenergy" is an open access journal, meaning that the full-text of all published articles is made freely available on the journal's website with no subscription or registration barriers.

If you would like to order reprints of this article please click here, <https://www.hindawi.com/journals/ijp/2021/4033692/reprint/>.

Best regards,

Marina Adel  
International Journal of Photoenergy  
Hindawi  
<https://www.hindawi.com/>

## Research Article

# Fabrication of Dye-Sensitized Solar Cells (DSSC) Using Mg-Doped ZnO as Photoanode and Extract of Rose Myrtle (*Rhodomyrtus tomentosa*) as Natural Dye

Nurdin Siregar <sup>1</sup>, Motlan,<sup>1</sup> Jonny Haratua Panggabean,<sup>1</sup> Makmur Sirait <sup>1</sup>,  
Juniastel Rajagukguk <sup>1</sup>, Noto Susanto Gultom <sup>1</sup> and Fedlu Kedir Sabir <sup>2</sup>

<sup>1</sup>Department of Physics, Faculty of Mathematics and Natural Sciences, State University of Medan, Jl. Willem Iskandar Pasar Medan Estate, Medan 20221, Indonesia

<sup>2</sup>Department of Applied Chemistry, School of Applied Natural Science, Adama Science and Technology University, P.O. Box 1888, Adama, Ethiopia

Correspondence should be addressed to Nurdin Siregar; [siregarnurdin@unimed.ac.id](mailto:siregarnurdin@unimed.ac.id)

Received 6 April 2021; Revised 29 June 2021; Accepted 21 August 2021; Published 3 September 2021

Academic Editor: Joaquim Carneiro

Copyright © 2021 Nurdin Siregar et al. This is an open access article distributed under the Creative Commons Attribution License, which permits unrestricted use, distribution, and reproduction in any medium, provided the original work is properly cited.

A dye-sensitized solar cell (DSSC) device using Mg-doped Zn thin films as photoanode and fruit extract of rose myrtle (*Rhodomyrtus tomentosa*) as the natural dye was investigated. The effect of annealing temperature (400–550°C) on the films of photoanode was systematically studied using an X-ray diffractometer (XRD), UV-Visible Near Infrared (UV-Vis NIR) Spectrophotometer, scanning electron microscopy (SEM), and energy dispersive spectroscopy (EDS). XRD confirm that all sample has the wurtzite hexagonal with crystallite size of 25 nm. The SEM images reveal particles on the surface of the Mg-doped ZnO thin film of irregular shapes. Increasing the annealing temperature leads to a larger particle size and slightly increases bandgap energy. The dye sensitizer of extracted rose myrtle (*Rhodomyrtus tomentosa*) has a strong absorption at the visible light region. The maximum efficiency of the DSSC device is 3.53% with Mg-ZnO photoanode annealed at 500°C.

## 1. Introduction

The demands for renewable energy continually increase every year due to its eco-friendliness. Solar cells have been well known as a device to convert solar energy to electricity for decades. However, conventional solar cells are still high priced due to complicated fabrication process and expensiveness of raw materials. Dye-sensitized solar cell (DSSC) is one of the most promising solar cell types to produce renewable energy with a low-cost material and simple fabrication process [1–3]. After irradiation, the dye sensitizer harvests light and causes an electron to promote the conduction band leaving a hole in the valence band. There are numerous pigments of plant leaves, fruits, and flowers that have the potential to be utilized in DSSC. The variety of pigments with different absorption wavelengths and degrees of absorptivity in the UV-visible spectrum can cause different performances of

DSSC. The molecules of the dye can be anchored into the surface areas of the semiconductor to form Lewis acid-base types of interaction to enhance electron transfer from HOMO of the dye molecule (pigment) to the conduction band of the semiconductor (anode) [4–7].

Zinc oxide (ZnO) semiconductor plays an important role as a photoanode to improve the conducting interface layer and to enhance the power conversion efficiency (PCE). According to the literature, ZnO has a high electron mobility, wide bandgap (3.37 eV), and large exciton binding energy of 60 meV [8]. Magnesium (Mg) is one of the metals that is used in many applications such as refractory materials and optical and heating apparatus [9, 10]. Mg-doped ZnO material also has special properties to block the electron due to its wide bandgap [11, 12]. There are several methods to grow thin film on a substrate, such as molecular beam epitaxy, metal-organic chemical vapor deposition, plasma-

enhanced chemical deposition, sputtering method, spray pyrolysis, atomic layer deposition, pulse laser deposition, electron beam evaporation, and sol-gel [13]. The sol-gel method has several advantages compared to the aforementioned methods such as simple, cheap, and efficient [14]. By using a sol-gel spin coating technique, several parameters like concentration of precursor solution, annealing temperature, and annealing time can be easily tuned in order to achieve the desired properties [12, 15].

In this work, the photoanodes of Mg-doped ZnO thin films were prepared by a sol-gel spin coating method. To the best of our knowledge, the natural dye from the fruit extract of *Rhodomyrtus tomentosa* has not been reported yet as the dye sensitizer for DSSC. The effect of different annealing temperatures on structural and optical properties of Mg-doped ZnO photoanodes as well as the efficiency of DSSC device was systematically investigated using necessary characterization tools. We find that the maximum efficiency of the DSSC device is 3.53% with Mg-doped ZnO photoanode annealed at 500°C.

## 2. Experimental Section

**2.1. Synthesis of Mg-Doped ZnO Thin Films.** Mg-doped ZnO thin films were fabricated using a sol-gel spin coating technique. Typically, zinc acetate dihydrate and magnesium chloride (2 wt.%) were dissolved in isopropanol (35 mL) under continuous stirring. After 10 min, 1.7 mL diethanolamine was added slowly into the solution. After refluxing process at 90°C for about 2 hours, the gel was dropped on top of FTO glass and spun at 5000 rpm for 60 s. After the drying process, the samples were annealed at different temperatures of 400, 450, 500, and 550°C for 5 hours.

**2.2. Extraction of Natural Dyes.** About 50 grams of *Rhodomyrtus tomentosa* fruit was ground using a mortar. After being moved into a beaker glass, 25 mL DI water, 21 mL ethanol, and 4 mL acetic acid were added and then stirred to form a homogeneous solution. The solution was then covered with aluminum foil to avoid photooxidation and soaked at room temperature for 24 h. Finally, the solid and liquid parts were separated using filter paper. The filtered solution of *Rhodomyrtus tomentosa* fruit extract was ready to be used as the sensitizer in DSSCs.

**2.3. Fabrication of DSSC.** Figure 1 illustrates the schematic fabrication of the DSSC device. First, the as-prepared Mg-doped ZnO thin film was used as the photoanode electrode. Natural dye sensitized from *Rhodomyrtus tomentosa* fruit extract was adsorbed on the top of Mg-doped ZnO photoanode by immersing it into the extracted dye solution for several hours. After that, it was taken out and washed with ethanol to remove the unadsorbed dye and dried in the oven at 80°C. The commercial platinum coated on the glass FTO was used as the counter electrode. The DSSCs were assembled by attaching the photoanode and the counter electrode using thermoplastic sealant surlyn as glue and separator and then heated at 80°C to let the surlyn perfectly attach to the electrodes. The electrolyte was injected through a tiny hole

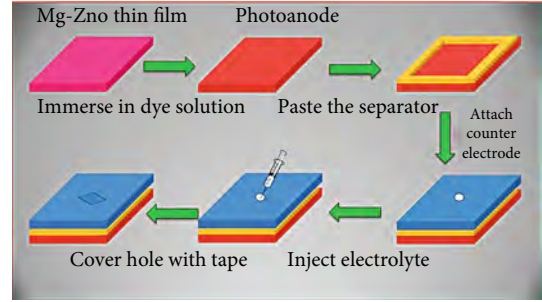


FIGURE 1: Schematic of the fabrication of DSSC using Mg-doped ZnO photoanode and fruit extract of *Rhodomyrtus tomentosa*.

that was drilled on the counter electrode. Finally, that hole was covered with transparent tape.

**2.4. Characterization Tools.** To observe the surface morphology of Mg-doped ZnO thin films annealed at different temperatures, a scanning electron microscope (JEOL-6500) analysis was performed at an accelerating voltage of 15 kV. The X-ray diffraction (XRD) pattern of Mg-doped ZnO thin films was analyzed using an X-ray diffractometer (LabX XRD-6100, Shimadzu) with Cu K $\alpha$  ( $\lambda = 1.54 \text{ \AA}$ ). The transmittance and absorbance spectra were recorded using a UV-Vis NIR spectrophotometer. The efficiency of the DSSC was measured using an I-V measurement (Keithley Source Measure Unit) system by irradiating a photoanode electrode with a LED and input power of 35 mW/cm<sup>2</sup>. Several data such as open-circuit voltage ( $V_{oc}$ ), short circuit current density ( $J_{sc}$ ), maximum voltage ( $V_{max}$ ), and maximum current ( $J_{max}$ ) were recorded. Then, the fill factor (FF) and efficiency ( $\eta$ ) were determined using equations (1) and (2), respectively.

$$FF = \frac{J_{max} \times V_{max}}{J_{sc} \times V_{oc}}, \quad (1)$$

$$\eta = FF \frac{J_{sc} \times V_{oc}}{P_{in}} \times 100\%. \quad (2)$$

## 3. Results and Discussion

**3.1. Electron Microscope Analysis.** The surface morphology of Mg-doped ZnO with variation of annealing temperatures was investigated using a field-emission scanning electron microscope. With a magnification of 30k times, the top view images of Mg-doped ZnO thin films can be clearly observed in Figure 2. The surface microstructure of Mg-doped ZnO at different annealing temperatures shows nanoparticles with irregular shapes. It was clearly observed that by increasing the annealing temperature, the particle size was monotonically increased. Figure 2(d) shows the representative energy dispersive spectroscopy (EDS) spectra. The spectra exhibit five peaks to indicate the presence of zinc, oxygen, magnesium, platinum, and tin in the film. The appearance of platinum is contributed from the platinum coating before SEM analysis to improve the conductivity while tin comes from the substrate. The presence of a relatively low-intensity peak

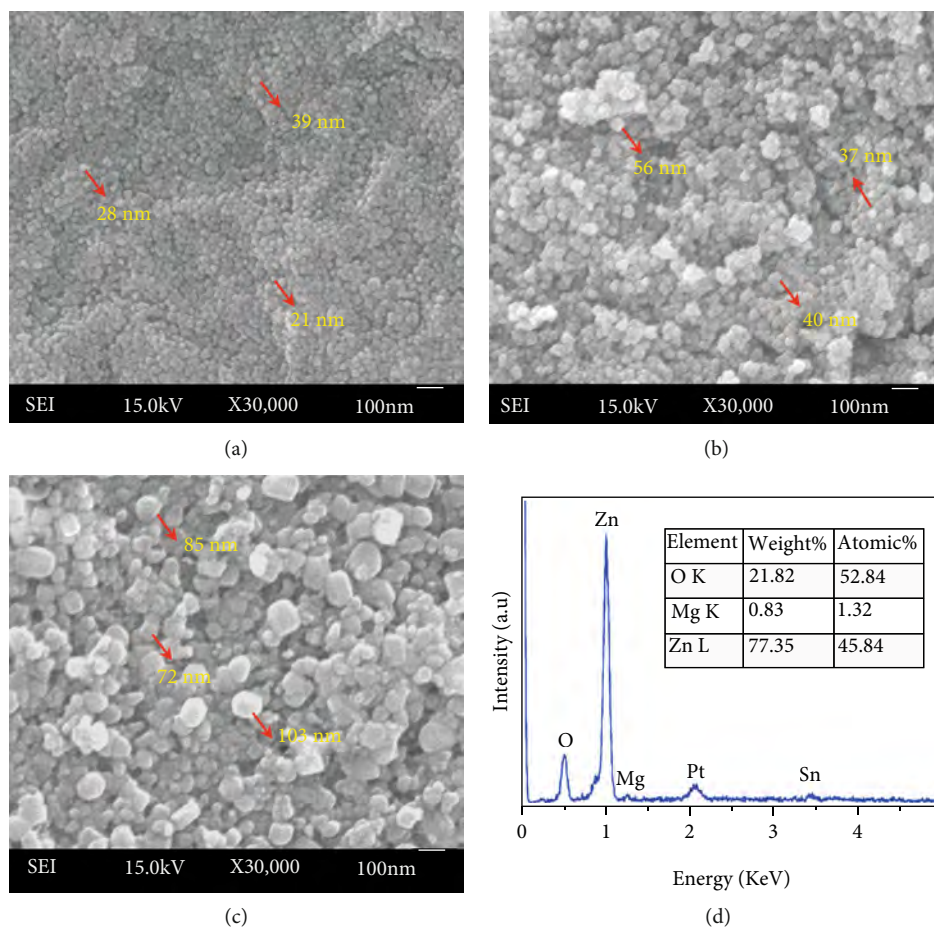


FIGURE 2: Scanning electron microscope images of Mg-doped ZnO with variation of annealing temperatures: (a) 400, (b) 500, (c) 550, and (d) representative EDS analysis.

for Mg compared to zinc and O peaks confirmed the successful Mg doping into ZnO host. Furthermore, the EDS quantitative result depicted in Figure 2(d) has shown that the weight and atomic percentage of Mg are about 0.83 and 1.32%, respectively.

To calculate the particle size more precisely, further analysis was conducted using ImageJ analysis. As shown in Figures 3(a)–3(c), the average particle sizes for Mg-doped ZnO thin films annealed at 400, 500, and 550°C are  $30 \pm 5$ ,  $53 \pm 9$ , and  $82 \pm 17$  nm, respectively. A larger particle size at a higher annealing temperature was reasonable. It could be explained due to a higher driving force from thermal energy that leads to a faster particle growth through Ostwald ripening mechanism. Our findings also well agree with some previous reports [16, 17].

**3.2. XRD Analyses.** The crystal properties of Mg-doped ZnO were studied by the XRD technique. The results are shown in Figure 4. The XRD patterns are similar to a wurtzite crystal structure based on the standard card of JCPDF #36-1451 (ZnO) [18]. Three peaks that located at  $32.5^\circ$ ,  $35.3^\circ$ , and  $37.0^\circ$  for  $2\theta$  could be assigned as (100), (001), and (101) planes of ZnO, respectively. The other weak peak at about  $38.5^\circ$  might be contributed by impurity as reported in the previous work [19]. The intensity of peaks in Figure 4 grad-

ually elevates as the temperature of annealing increases, which indicates an improvement in the crystallinity of Mg-doped ZnO films.

Table 1 lists the summary of structural properties of Mg-doped ZnO thin films at different annealing temperatures. The average crystallite size of Mg-doped ZnO thin films was calculated at (101) plane using the Scherrer formula as shown in equation (3) [20]. Their crystallite size values are 20.60, 21.23, 16.83, and 22.9 nm at the annealing temperature of 400, 450, 500, and 550°C, respectively. Next, the dislocation density ( $\delta$ ) of Mg-doped ZnO was further determined by equation (4) [21]. The dislocation density of Mg-doped ZnO annealed at 400, 450, 500, and 550°C is  $2.36 \times 10^{-3}$ ,  $2.22 \times 10^{-3}$ ,  $3.53 \times 10^{-3}$ , and  $1.89 \times 10^{-3} \text{ nm}^{-2}$ , respectively. Mg-doped ZnO annealed at 500°C has the highest dislocation density compared to other samples. Macrostrain value that indicates the peak shift position was calculated according to equation (5) [22]. Based on the database, the (101) plane for ZnO is located at  $36.25^\circ$  with an interplanar spacing of 2.4759 Å. However, the (101) plane for our Mg-doped ZnO is found at about  $37.00^\circ$  for  $2\theta$  with a calculated interplanar spacing of 2.4272 Å. The peak shifting of about  $0.75^\circ$  for  $2\theta$  also indicates that Mg as a dopant has been successfully doped into ZnO host lattice [23]. The macrostrain value was similar for different temperatures

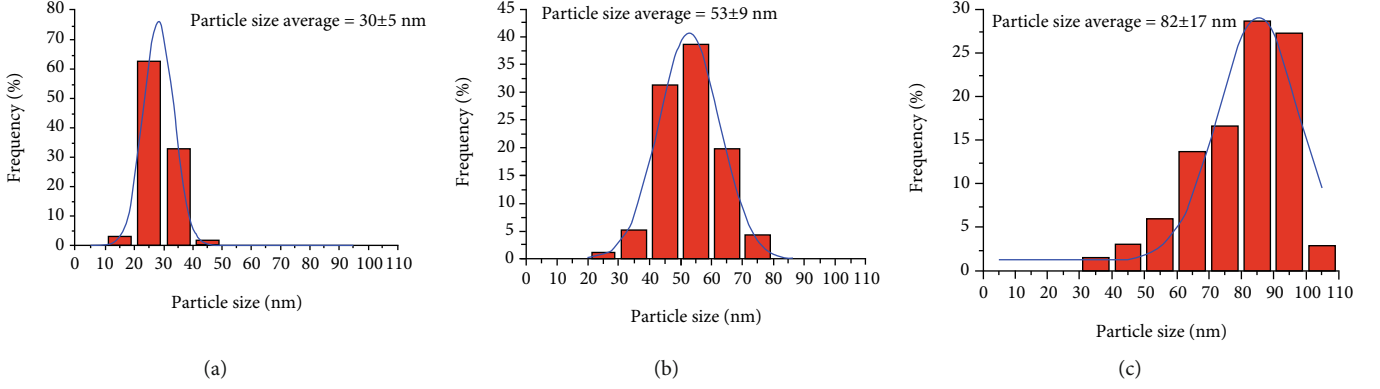


FIGURE 3: Particle size distribution of Mg-doped ZnO annealed at (a) 400, (b) 500, and (c) 550°C.

with a value of  $1.97 \times 10^{-2}$  because of their similarity in peak position. Based on the previous reports [24], the lattice parameters  $a$  and  $c$  of Mg-doped ZnO were estimated to be about 3.172 Å and 5.080 Å using equations (6) and (7), respectively. The lattice parameter  $a$  at the (100) plane did not significantly differ for different annealing temperatures because their peak position was located almost in the same diffraction angle. Similarly, the lattice parameter  $c$  at the (002) plane is also very similar at different annealing temperatures, as listed in Table 1.

$$D = \frac{0.9\lambda}{\beta \cos \theta}, \quad (3)$$

where  $D$  is the crystallite size (nm),  $\lambda$  is the wavelength (nm),  $\beta$  is the full half maximum, FWHM (rad), and  $\theta$  is the Bragg angle (°).

$$\delta = \frac{1}{D^2}, \quad (4)$$

$$\langle e \rangle = \frac{d - d_o}{d_o}, \quad (5)$$

where  $d_o$  is the interplanar spacing of pure ZnO without deformation while  $d$  is the calculated interplanar spacing for Mg-doped ZnO at the (101) plane using the Bragg law.

$$a = \frac{\lambda}{\sqrt{3} \sin \theta_{(100)}}, \quad (6)$$

$$c = \frac{\lambda}{\sin \theta_{(002)}}. \quad (7)$$

**3.3. Optical Properties.** To study the effect of different annealing temperatures on optical properties, the absorption and transmission spectra of Mg-doped ZnO thin films are measured and presented in Figures 5 and 6, respectively. The absorption peaks of all Mg-doped ZnO thin films are located at a wavelength of 350 nm, which is at the UV region. As clearly shown in Figure 5, the absorption of Mg-doped ZnO annealed at 400°C is quite low. However, after increasing the annealing temperature to 450°C and

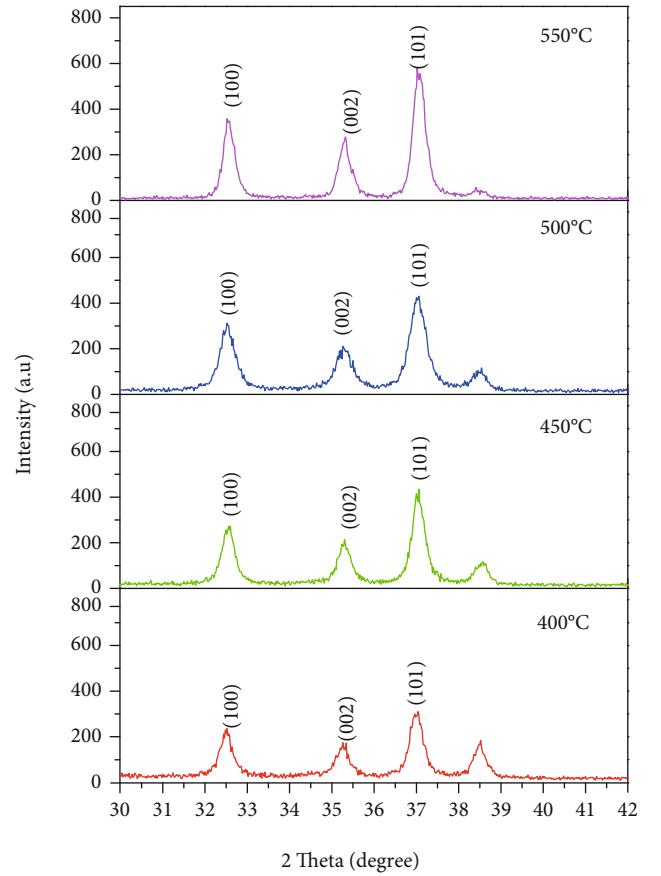


FIGURE 4: XRD pattern of Mg-doped ZnO thin films at different annealing temperatures.

500°C, the absorption sharply elevates. Further increasing the temperature of annealing to 550°C leads to a lower absorbance but is still higher than that at 400°C. Figure 6 exhibits transmission spectra of Mg-doped ZnO which also shows a similar trend to the absorption spectra in Figure 5. The thin films have transparency about 50-80% at visible light region.

The bandgap energy of Mg-doped ZnO thin films was further derived based on the optical absorption data and plotted in Figure 7. As listed in Table 2, bandgap energy values are 3.20, 3.24, 3.30, and 3.33 eV for annealing at



TABLE 1: Summary of crystal properties of FWHM, crystallite size, dislocation density, macrostrain values, and lattice parameters ( $a$  and  $c$ ) of Mg-doped ZnO thin films at different annealing temperatures.

Temperature (°C)	FWHM/ $\beta$ (rad)	Crystallite size (nm)	Dislocation density $\times 10^{-3}$ (nm $^{-2}$ )	Macro strain values $\langle e \rangle$	Lattice parameters (Å)	
					$a$	$c$
400	0.4065	20.60	2.36	$1.97 \times 10^{-2}$	3.176	5.082
450	0.3945	21.23	2.22	$1.97 \times 10^{-2}$	3.172	5.080
500	0.4976	16.83	3.53	$1.97 \times 10^{-2}$	3.175	5.083
550	0.3645	22.9	1.89	$1.97 \times 10^{-2}$	3.173	5.080

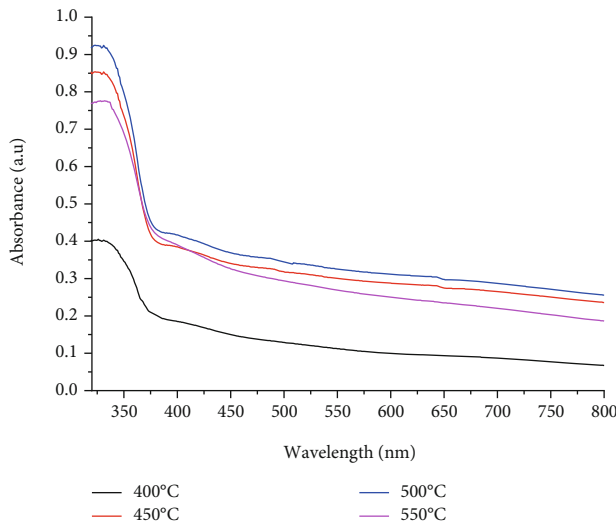


FIGURE 5: Absorbance spectra of Mg-doped ZnO thin films at different annealing temperatures.

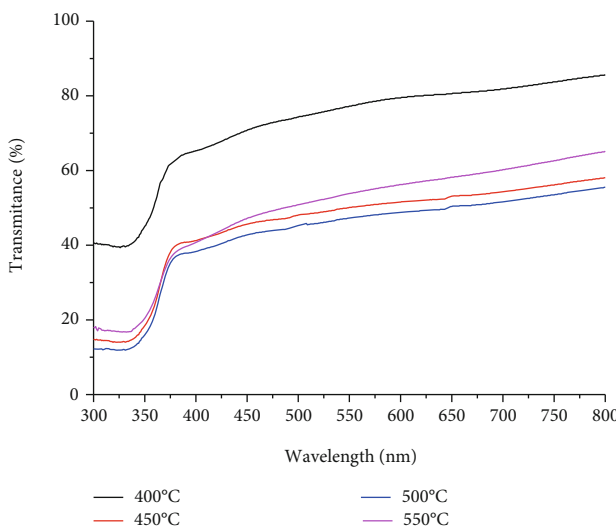


FIGURE 6: Transmittance spectrum of Mg-doped ZnO thin films at different annealing temperatures.

400, 450, 500, and 550°C, respectively. The slight increment of bandgap energy with increasing temperature might be due to the Burstein–Moss effect as reported in previous studies [25].

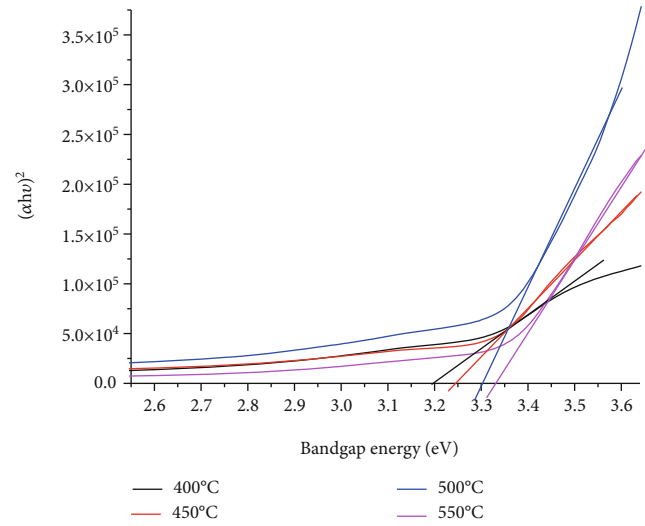


FIGURE 7: Tauc plot of Mg-doped ZnO thin films at different annealing temperatures.

TABLE 2: Bandgap energy of Mg-doped ZnO thin film at different annealing temperatures.

Temperature (°C)	Bandgap energy (eV)
400	3.20
450	3.24
500	3.30
550	3.33

**3.4. Absorbance of *Rhodomyrtus tomentosa* Dye Extract.** The optical absorption spectrum of the extracted rose myrtle (*Rhodomyrtus tomentosa*) natural dye was measured using a UV-Vis spectrophotometer to investigate its sensitivity to light. As shown in Figure 8, the natural dye has a strong absorption at the visible-light region with an intense absorbance peak at a wavelength of 610 nm. This property is very useful for DSSC to improve the light absorption ability. It is also well known that about 43% of the solar spectrum falls in the visible light range and only 4% is in the UV region [26]. The more light can be absorbed, the more electron-hole can be generated, which leads to a higher efficiency of a DSSC device.

**3.5. Efficiency of DSSC.** Figure 9 exhibits the  $J - V$  characteristic curve of DSSC with Mg-doped ZnO as photoanode at

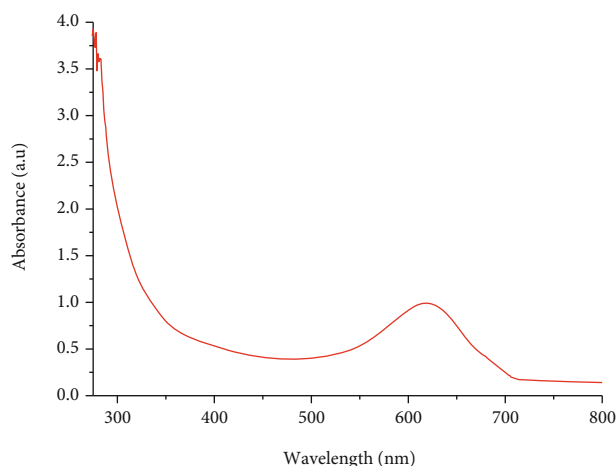


FIGURE 8: Absorbance spectrum of natural dye of extracted rose myrtle (*Rhodomyrtus tomentosa*).

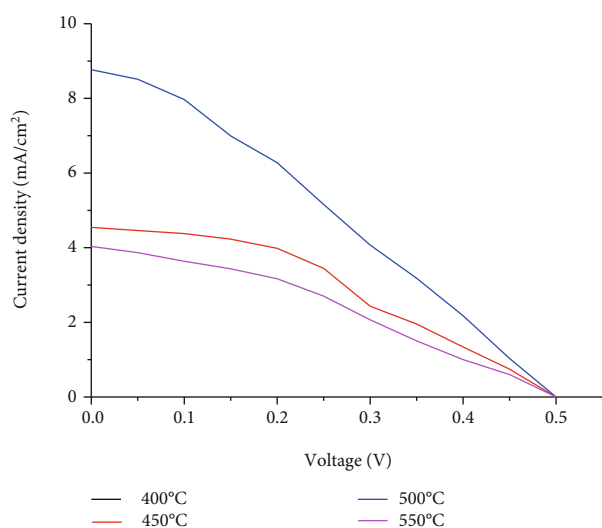


FIGURE 9:  $J - V$  characteristic curve of DSSC using Mg-doped ZnO as photoanode at different annealing temperatures.

TABLE 3: Summary of electrical properties including open-circuit voltage, short-circuit current, fill factor, and efficiency of DSSC for different annealing temperatures.

Temperature (°C)	$V_{oc}$ (V)	$J_{sc}$ (mA/cm <sup>2</sup> )	$P_{max}$ (mW/cm <sup>2</sup> )	FF (%)	$\eta$ (%)
400	0.5	3.83	0.61	31.70	1.66
450	0.5	4.55	0.86	37.93	2.36
500	0.5	8.77	1.29	29.42	3.53
550	0.5	4.03	0.68	33.47	1.85

different annealing temperatures and the fruit extract of *Rhodomyrtus tomentosa* as a natural dye sensitizer. Further, the photovoltaic properties of DSSC are listed in Table 3. The open-circuit voltage ( $V_{oc}$ ) at different annealing temperatures was similar with a value of 0.5 V. In contrast, the short-circuit current ( $J_{sc}$ ) was significantly different. The  $J_{sc}$  values are 3.83, 4.55, 8.77, and 4.03 mA/cm<sup>2</sup> at annealing

temperatures of 400, 450, 500, and 550°C, respectively. The efficiency of the DSSC device annealed at 400°C was about 1.66%. By increasing the annealing temperature to 450°C, the efficiency also was increased to 2.36%. Further increasing the annealing temperature to 500°C, the efficiency of 3.53% can be achieved. However, the efficiency was observed to decline when the annealing temperature is 550°C. Therefore, the optimum annealing temperature is 500°C with a maximum power conversion efficiency of 3.53%. Based on the characterization results, the highest efficiency of 3.53% at 500°C could be contributed due to its highest optical absorption as revealed by UV-Vis analysis in Figure 5.

## 4. Conclusions

We have successfully fabricated a dye-sensitized solar cell (DSSC) device using Mg-doped ZnO thin film as the photoanode and natural dye of rose myrtle (*Rhodomyrtus tomentosa*) as the dye sensitizer. The scanning electron microscope analysis revealed that the surface of Mg-doped ZnO thin film was particles with irregular shapes. It is found that increasing the annealing temperature led to a larger particle size and slightly increased bandgap energy. The natural rose myrtle dye sensitizer had a strong absorption at the visible light region. The maximum efficiency of the DSSC device was 3.53% at an annealing temperature of 500°C. This work demonstrates that the annealing temperature of photoanode significantly affects the efficiency of the DSSC device.

## Data Availability

The research data used to support the findings of this study are included in the article.

## Conflicts of Interest

The authors declare that they have no conflicts of interest.

## Acknowledgments

The authors would like to thank the Rector of Universitas Negeri Medan for supporting this research.

## References

- [1] J. Gong, J. Liang, and K. Sumathy, "Review on dye-sensitized solar cells (DSSCs): fundamental concepts and novel materials," *Renewable and Sustainable Energy Reviews*, vol. 16, no. 8, pp. 5848–5860, 2012.
- [2] T.-L. Wu, T. H. Meen, S. M. Chao et al., "Application of ZnO micro rods on the composite photo-electrode of dye sensitized solar cells," *Microsystem Technologies*, vol. 24, no. 1, pp. 285–289, 2018.
- [3] R. Vittal and K.-C. Ho, "Zinc oxide based dye-sensitized solar cells: a review," *Renewable and Sustainable Energy Reviews*, vol. 70, pp. 920–935, 2017.
- [4] E. T. Bekele, E. A. Zereffa, N. S. Gultom, D.-H. Kuo, B. A. Gonfa, and F. K. Sabir, "Biotemplated synthesis of titanium oxide nanoparticles in the presence of root extract of *Kniphofia schemperii* and its application for dye sensitized solar cells,"

- International Journal of Photoenergy*, vol. 2021, Article ID 6648325, 12 pages, 2021.
- [5] U. Mehmood, S.-u. Rahman, K. Harrabi, I. A. Hussein, and B. V. S. Reddy, "Recent advances in dye sensitized solar cells," *Advances in Materials Science and Engineering*, vol. 2014, Article ID 974782, 12 pages, 2014.
- [6] S. Datta, A. Dey, N. R. Singha, and S. Roy, "Enhanced performance of dye-sensitized solar cell with thermally stable natural dye-assisted  $\text{TiO}_2/\text{MnO}_2$  bilayer-assembled photoanode," *Materials for Renewable and Sustainable Energy*, vol. 9, 2020.
- [7] M. Ye, X. Wen, M. Wang et al., "Recent advances in dye-sensitized solar cells: from photoanodes, sensitizers and electrolytes to counter electrodes," *Materials Today*, vol. 18, no. 3, pp. 155–162, 2015.
- [8] S. Sasidharan, S. Soman, S. C. Pradhan et al., "Fine tuning of compact ZnO blocking layers for enhanced photovoltaic performance in ZnO based DSSCs: a detailed insight using  $\beta$  recombination, EIS, OCVD and IMVS techniques," *New Journal of Chemistry*, vol. 41, no. 3, pp. 1007–1016, 2017.
- [9] M. Rashad, H. O. Tekin, H. M. H. Zakaly, M. Pyshkina, S. A. M. Issa, and G. Susoy, "Physical and nuclear shielding properties of newly synthesized magnesium oxide and zinc oxide nanoparticles," *Nuclear Engineering and Technology*, vol. 52, no. 9, pp. 2078–2084, 2020.
- [10] X. Fu, S. Jiao, Y. Jiang et al., "Large-scale growth of ultrathin low-dimensional perovskite nanosheets for high-detectivity photodetectors," *ACS Applied Materials & Interfaces*, vol. 12, no. 2, pp. 2884–2891, 2020.
- [11] D. Fang, C. Li, N. Wang, P. Li, and P. Yao, "Structural and optical properties of Mg-doped ZnO thin films prepared by a modified Pechini method," *Crystal Research and Technology*, vol. 48, no. 5, pp. 265–272, 2013.
- [12] F. Lekoui, S. Hassani, M. Ouchabane et al., "Elaboration and characterization of Mg-doped ZnO thin films by thermal evaporation: annealing temperature effect," *Brazilian Journal of Physics*, vol. 51, no. 3, pp. 544–552, 2021.
- [13] A. Jilani, M. Abdel-wahab, and A. Hammad, *Advance deposition techniques for thin film and coating*, 2017.
- [14] F. Aslan, A. Tumbul, A. Gökteş, R. Budakoğlu, and İ. H. Mutlu, "Growth of ZnO nanorod arrays by one-step sol-gel process," *Journal of Sol-Gel Science and Technology*, vol. 80, no. 2, pp. 389–395, 2016.
- [15] M. N. H. Mia, M. F. Pervez, M. K. Hossain et al., "Influence of Mg content on tailoring optical bandgap of Mg-doped ZnO thin film prepared by sol-gel method," *Results in Physics*, vol. 7, pp. 2683–2691, 2017.
- [16] M. Arif, A. Sanger, P. M. Vilarinho, and A. Singh, "Effect of annealing temperature on structural and optical properties of sol-gel-derived ZnO thin films," *Journal of Electronic Materials*, vol. 47, no. 7, pp. 3678–3684, 2018.
- [17] T.-H. Chen, M. W. Wang, C. L. Yang, and Y. S. Huang, "Effects of different annealing temperature on the optoelectrical properties of MGZO thin films prepared by co-sputtering method," *Microsystem Technologies*, vol. 25, no. 5, pp. 2109–2115, 2019.
- [18] N. S. Gultom, H. Abdullah, and D.-H. Kuo, "Phase transformation of bimetal zinc nickel oxide to oxysulfide photocatalyst with its exceptional performance to evolve hydrogen," *Applied Catalysis B: Environmental*, vol. 272, p. 118985, 2020.
- [19] J. L. Konne and B. O. Christopher, "Sol-Gel Syntheses of Zinc Oxide and Hydrogenated Zinc Oxide (ZnO:H) Phases," *Journal of Nanotechnology*, vol. 2017, Article ID 5219850, 8 pages, 2017.
- [20] N. S. Gultom, H. Abdullah, and D.-H. Kuo, "Facile synthesis of cobalt-doped (Zn,Ni)(O,S) as an efficient photocatalyst for hydrogen production," *Journal of the Energy Institute*, vol. 92, no. 5, pp. 1428–1439, 2019.
- [21] H. Ertap and M. Karabulut, "Structural and electrical properties of boron doped InSe single crystals," *Materials Research Express*, vol. 6, no. 3, 2019.
- [22] E. M. Al-Khalqi, M. A. A. Hamid, N. H. Al-Hardan, and L. K. Keng, "Highly sensitive magnesium-doped ZnO nanorod pH sensors based on electrolyte-insulator-semiconductor (EIS) Sensors," *Sensors*, vol. 21, no. 6, p. 2110, 2021.
- [23] M. A. Zeleke, D. H. Kuo, K. E. Ahmed, and N. S. Gultom, "Facile synthesis of bimetallic (In,Ga) $_2$ (O,S) $_3$  oxy-sulfide nanoflower and its enhanced photocatalytic activity for reduction of Cr(VI)," *Journal of Colloid and Interface Science*, vol. 530, pp. 567–578, 2018.
- [24] S. Kurtaran, "Al doped ZnO thin films obtained by spray pyrolysis technique: influence of different annealing time," *Optical Materials*, vol. 114, p. 110908, 2021.
- [25] A. Goktas, A. Tumbul, Z. Aba, and M. Durgun, "Mg doping levels and annealing temperature induced structural, optical and electrical properties of highly c-axis oriented ZnO:Mg thin films and Al/ZnO:Mg/p-Si/Al heterojunction diode," *Thin Solid Films*, vol. 680, pp. 20–30, 2019.
- [26] N. S. Gultom, H. Abdullah, J. C. Xie, and D. H. Kuo, "Transforming Zn(O,S) from UV to visible-light-driven catalyst with improved hydrogen production rate: effect of indium and heterojunction," *Journal of Alloys and Compounds*, vol. 869, p. 159316, 2021.